Seeing is Believing: In Situ/Operando Optical Microscopy for Probing Electrochemical Energy Systems

Binbin Chen,* Hao Zhang, Jin Xuan,* Gregory J. Offer, and Huizhi Wang

This review discusses a range of in situ/operando techniques based on optical microscopy reported in literatures for studying electrochemical energy systems. Compared to other techniques (scanning probe microscopy, electron microscopy, X-ray microscopy), optical microscopy offers many advantages including the simplicity of the instrument and operation, cost effectiveness, and nondestructive nature. In the past few decades, significant advances in the field of optical microscopy have been made, enabling new opportunities of more elaborate studies on electrochemical energy systems. Herein, different methodologies are compared, with the emphasis on experimental setup designs and findings, to illustrate their aptness.

1. Introduction

Energy storage plays a crucial role in the future sustainable energy systems, considering the needs to balance the output fluctuations of renewable energy sources and support the prosperities of electronic devices and electric transportation.[1,2] Of various storage methods, electrochemical storage are a choice to meet the various energy demands of the society.[3,4] Over the past decades, great efforts have been made to optimize electrochemical energy systems (EESs) in terms of energy and power densities, lifespan, safety and costs, which are dependent on their internal physico-chemical processes such as redox reactions, ion transports, formation of interstitial interfaces, degradation of components and by-substances

generation.[5] Understanding the mechanisms and fundamentals inside the EESs are critical to improve their performances by boosting the favorable processes and suppressing the detrimental ones.

Various ex situ techniques have been used for studying EESs, which provide valuable spatial and temporal information.[6–8] Nevertheless, ex situ methods are limited by the time delay and potential impacts during the operation of removing samples from their initial environments to characterization locations.[9] The results might sometimes be missing or even misleading. This elicits the requirement for in situ/operando methods to conduct real-time observations on reactions and processes inside a system. In situ analytical techniques can provide more realistic information on the ongoing chemical and physical processes in an electrochemical cell.[10] Furthermore, correlating in situ information with electrochemical results obtained synchronously from the same device enables to build a direct cause-and-effect relationship, leading to authentic conclusions.[11]

Remarkable progress has been made with advanced characterization techniques including optical,[12] X-ray,[13] electron microscopy,[14] neutron techniques.[15] The techniques work on very different principles. Optical microscopy is based on transmitting light to construct images for the samples. It has a wide effective characterization scales from centimeter to lower than micrometer. X-ray characterization techniques utilize electromagnetic radiation to magnify the samples. X-ray methods, including diffraction, absorption spectroscopy, photoelectron spectroscopy and X-ray microscopy, provide crucial information from mesoscale morphology to microscale crystal structure and elemental content of electrode materials.[16] Electron microscopy probes the samples with electron beams.[17] The techniques based on neutron are quite similar as electron, and neutrons are preferable for analyses of light elements such as lithium ion (Li+). Also, Neutrons can go in more penetration depth with a weaker interaction with matter.[18] With the employment of these techniques, the knowledge of mechanisms of EESs has been significantly enhanced. On the other hand, in situ/operando experiments are restricted under certain circumstances, as they generally require special designs and modifications of the unit structures. Compared with other techniques, optical microscopy is preferable for in situ/operando studies considering the basic equipment needed, nonvacuum manipulation, easy access and operation, as well as its nondestructive nature.[19] However, inspections based on optical microscopy require access within the systems for transmitting light.

Dr. B. Chen, Dr. G. J. Offer, Dr. H. Wang
Department of Mechanical Engineering
Imperial College London
London SW7 2AZ, UK
E-mail: b.chen@imperial.ac.uk

Dr. H. Zhang
School of Engineering
University of Edinburgh
Edinburgh EH9 3FB, UK

Prof. J. Xuan
Department of Chemical Engineering
Loughborough University
Loughborough LE11 3TU, UK
E-mail: j.xuan@lboro.ac.uk

The ORCID identification number(s) for the author(s) of this article can be found under https://doi.org/10.1002/admt.202000555.

ADVANCED
SCIENCE NEWS
www.advancedsciencenews.com

ADVANCED
MATERIALS
TECHNOLOGIES
www.advmattechnol.de

In recent decades, several advanced techniques have been proposed, which provide new opportunities for researchers to conduct in situ/operando studies in EESs. There have been several reviews of general in situ methods for EES,[20–22] none of which focused optical microscopy. Herein, we present a comprehensive review on in situ/operando optical microscopy for probing electrochemical energy systems. This review covers the working principles of optical microscopy, designs of in situ/operando electrochemical cells, major findings from the literatures and future research opportunities.

2. History and Development of Optical Microscopy Techniques

The operation of an optical microscope relies on the reflection and refraction of transmitting light on an object.[23] Hans and Zacharias Janssen created the first microscope composed of a compound design with eyepiece and objective lens in the 16th century.[24] Further improvements were made by Robert Hooke and Antonie van Leeuwenhoek. Each of them developed their own microscopes. Hooke, who was famed for his micrographic publications of vermin, expanded the size of magnification to approximately 30× based on Janssen's microscope.[25] Van Leeuwenhoek further increased the magnification of up to 300×. He has for the first time observed "animalcules" in pond water and human mouth. He also described microscopic findings of cellular structure including muscle fibers, white and red blood cells and spermatozoa.[26] In the late 19th century, Ernst Abbe, an optical theorist in Zeiss, put substantial efforts in reinforcing the magnifying capability of microscopes. He developed a theoretical understanding of the inherent limit of resolution of microscopes and found that the resolution is determined by the wavelength of light and the numerical aperture of the lens.[27] In collaboration with a glass chemist Otto Schott, Abbe achieved a spatial resolution of about half the wavelength of light by using a water immersion technique. Furthermore, Zeiss and Abbe enabled the manufacturing of affordable microscopes, which significantly brought down the costs and broadened the applications of optical microscopy.[28]

Following those early efforts on microscopes, Frits Zernicke developed the first phase contrast microscope that measured phase shifts. The phase contrast microscope has enabled the visualization of transparent live cells with increased contrast by illuminating light though the samples.[29] This technique has been widely adopted since the War II, and was award the 1953 Nobel Prize in Physics. Before the invention of the phase contrast microscope, fluorescent properties of substances had been investigated, and some substances had been found to emit light of longer wavelength than the illuminating light.[30,31] Based on this phenomenon, Oskar Heimstädt developed the first fluorescence microscope in 1910. However, Heimstädt himself was uncertain about the significance of fluorescence microscopy.[32] Meanwhile in the biology field, a variety of fluorescent probes have been synthesized specifically for the application of cell research including fluorescently labeled antibodies,[33] reactive dyes and the family of green fluorescent proteins.[34] With further settling for the limitation of background signal, the fluorescent microscope has become an indispensable tool for cell biologists.

Table 1. A brief summary of practical applications of optical microscopy.

Applications	Characterizations
Optical microscope	Direct eye observation: from mesoscale to microscale;
	Digital Camera: image processing, live tracking, digitalization;
Fluorescent microscope	Fluorescent dye: labeling and marking;
Optical Fiber	Bypass opaque medium of EESs;
Multibeam optical sensing	Deformation such as inflection, expansion, etc.;
Microparticle image velocimetry	Flow visualization for fluidics.

In 1961, Marvin Minsky proposed the concept of confocal microscopy by integrating two pinholes into the microscope.[35] Together with the advent of the lasers, the first scanning confocal microscopy became available in 1987. As the digital age began in 1980s, most technologies are digital-oriented. Digital microscopes, with a substitution of oculars with digital cameras and monitors, helped researchers record all the results and data easily, and the optical microscopy took off. Meanwhile, new techniques and applications such as optical fiber, multibeam optical sensing, etc., have been developed. With the development of more elaborate optical components and advanced designs, the aptness of optical microscopy has been greatly boosted as shown in **Table 1**.

Optical fiber was invented over one-hundred years ago. Lights from one end can transfer within the fiber core by total internal reflection till the other end even when the fiber is bending. Except for its momentous applications in the communication area, optical fiber is also helping microscopist to bypass the opaque barrier and transiting light into internal cavities.

With its unique propagation and reflection properties, light beam has been a very powerful tool for monitoring changes in the surface morphologies. Laser deflection technique, for example, can deduce the substrate curvature change by detect the position shift of a reflected laser beam.[36] Multibeam optical sensing technique was developed from laser deflection method by Floro et al in 1996 with higher resolution.[37] It has already proven successful in the applications of monitoring the stress-related phenomena in metal or thin films during chemical vapor deposition or molecular beam epitaxy.[38]

3. Optical Microscopy Studies of Polymer Electrolyte Membrane Fuel Cells (PEMFCs)

Benefiting from multiple advantages, such as, room temperature operation, high efficiency, fast start-up, and environmental friendliness, PEMFCs have been an attractive power source for automotive and stationary applications.[39] A PEMFC consists of a polymer electrolyte membrane, an anode and a cathode with porous layers to facilitate the transport of reactants to/products away from the catalyst surface and bipolar plates containing gas flow channels as shown in **Figure 1**.

Hydrogen is the most commonly used fuel in PEMFCs. In a hydrogen-fuelled PEMFC, hydrogen and oxygen react separately at individual electrodes, producing electricity, heat and
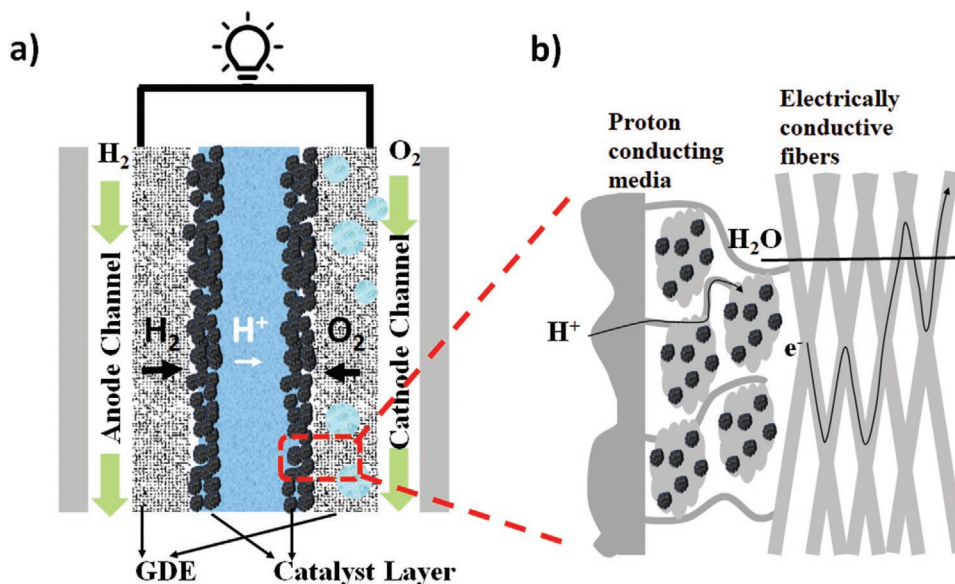
Figure 1. a) Schematic of a PEMFC illustrating the main components and operation principle. b) Schematic of a close-up on the cathode side of the membrane electrode assembly (MEA) showing the triple-phase boundary.

water. During the operation, water is formed at the cathode. Also, water vapor in the anode flow tends to migrate to the cathode along with protons (H^+) moving across the membrane under the electro-osmotic force. Hence, the water content on the cathode side is usually higher than that on the anode side. Meanwhile, a backward diffusion of water from the cathode to the anode through the membrane electrode assembly also takes place due to the water activity gradient. The ionic conductivity of the polymer electrolyte membrane and reactant transport are highly dependent on the water content. It would impose negative effects on mass and charge transfer if the level of water content hasn't been kept in a suitable range.[40] Therefore, proper water management is vital to ensure proper performance of fuel cells and prevent fuel cells from flooding and drying out. Water and mass transport is tightly coupled with heat transfer, hence, thermal management is also crucial to fuel cells.[41] Future development of PEMFCs requires a comprehensive understanding of these processes. Direct visualization techniques can provide the real-time information of internal distributions in an operating fuel cell and thus a useful platform for understanding PEMFCs.

3.1. Two-Phase Flow in Gas Channels

As one of the main challenges, the water management has been the subject under extensive investigations. The generation, accumulation, as well as the discharge of liquid water inside the electrodes need to be studied for better understanding of water transport in PEMFCs. Conventional optical photography has been employed widely to visualize liquid water transport in PEMFCs due to its simplicity. Through this methodology, its spatial and temporal resolution capabilities have helped to observe the water motion inside the flow channels, although internal visualization can be restricted by opacity of electrodes. Specially designed transparent cells have been developed to observe the surface of cell structures.

For optical analyses, transparent fuel cell designs are normally used to allow visualization of the interior of gas channel. A transparent cell consists of a conventional core MEA sandwiched between two transparent cover plates. The transparent cover plates are either made of stable transparent materials such as plexiglass or at least have a transparent glass window as shown in **Figure 2**. Taking advantage of these cell designs, the build-up, accumulation and discharge of liquid water on both anode and cathode surfaces have been studied. It was found that the build-up and accumulation of water on the electrode surface happen rapidly. Klaus et al. spotted water droplets inside the diffusion layer and water accumulation on the surfaces near the air inlet and outlet after 3 min of operation at a voltage of 500 mV.[42] Discrete water droplets were found to grow and form slugs in the channel and then eventually become plugs moving toward the outlet pushed by the gas flow. As the access of reactant gases was blocked by water, the cell voltage was observed to drop and rise as the blockage was expelled or broke up. The process happens periodically, causing a "V" shape appearance in the profile of the voltage.[43]

The two-phase flow in gas channels can be affected by factors such as flow rate, humidity,[43,45] channel dimensions and profiles (parallel, serpentine, and interdigitated),[46,47] temperature, current density,[48] gas diffusion layer (GDL) materials,[49] and gravitational orientations.[50] Zhan et al. found that the generation of water on the electrode is not uniform with a higher production rate under the channel backs than that in channel. Also, the water near the channel walls can easily form water film due to the capillary effect. In contrast, the liquid water on the GDL is near sphere drop since the surface of GDL is hydrophobic. The wettability on different materials have also been studied.[51] Parallel and serpentine channel presents a great difference in discharging liquid water. Once channels in parallel were blocked by water, the water can hardly move forward from the original spot and keeps blocking the channel. In comparison, serpentine channel shows rapid removal of water
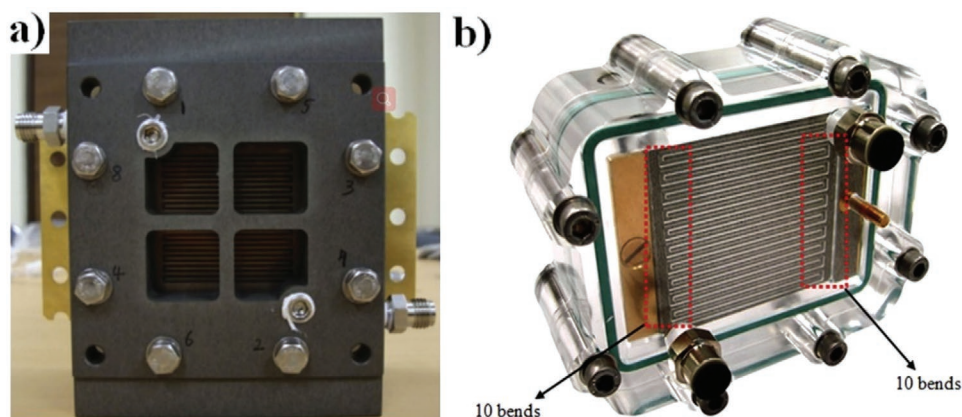
Figure 2. Transparent PEMFC setup: a) with a transparent observation window. Reproduced with permission.[43] Copyright 2011, Hydrogen Energy Publications. b) Whole transparent cover plates. Reproduced with permission.[44] Copyright 2017, Elsevier Ltd.

droplets. The water obstructs the gas transport into the electrode, as a result, the electrode cannot work effectively in these parts.[52]

It is noticed that most of the early visualization studies were limited to qualitative descriptions of water in forms of droplets, slugs and films within the gas channels. More attention should be paid to gathering quantitative data. Benefiting from high-resolution digital cameras and an increasing computing power, quantitative characterization of two-phase flows in fuel cells has become possible. Based on a visualization study of liquid water in straight channels on the cathode side, which were carried out on the surfaces in a range of humidity levels, Hussaini et al. quantitatively concluded the flow patterns into a flow map, in terms of two-phase pressure drop coefficient, voltage loss and wetted area ratio.[53] It was found that the

actual distribution of water depends on channel designs and experimental conditions, however, the value of the wetted area ratio was found to be fairly constant, indicating that it represented a certain working status of the cell, under a given set of operation conditions.

Sergi et al. further developed a technique using digital video processing to quantitatively measure the liquid water transport in gas channels covered by a transparent window.[54,55] The digital processing algorithm, as shown in **Figure 3**, was able to give more accurate results compared with manual selection processes. A dual-visualization setup was implemented to observe flow fields on both electrodes simultaneously during cell operation. The wetted area ratio was automatically calculated and the liquid water content was quantified in the flow fields.
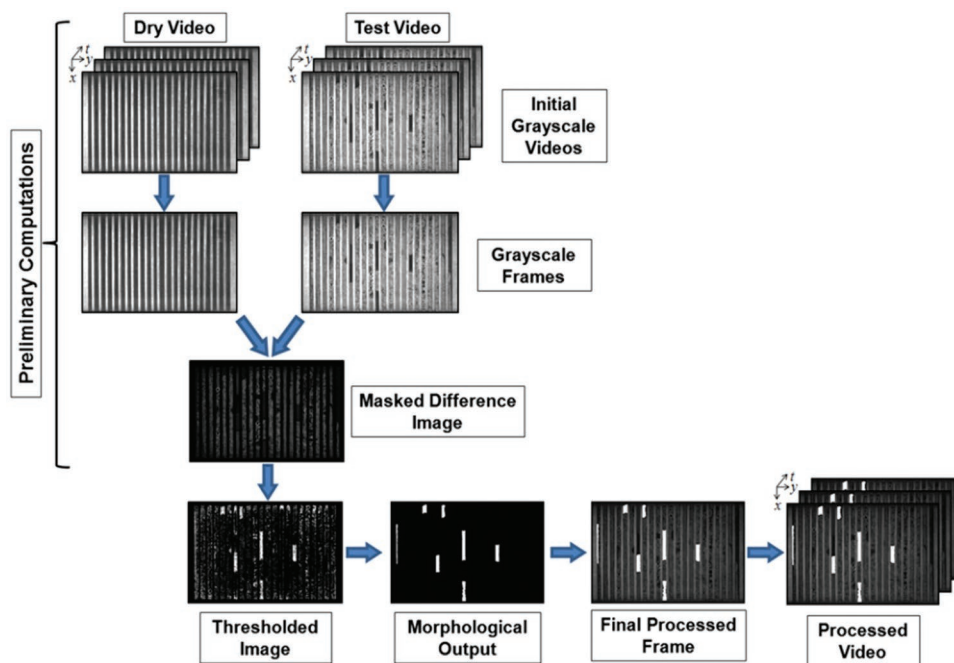
Figure 3. Digital data processing for water coverage ratio. Reproduced with permission.[55] Copyright 2011, Hydrogen Elsevier Ltd.

**ADVANCED
SCIENCE NEWS**

www.advancedsciencenews.com

**ADVANCED
MATERIALS
TECHNOLOGIES**

www.advmattechnol.de

New algorithms with MATLAB to quantitatively identify and measure the water flow patterns in frames captured by CCD were developed by Banerjee et al.[56] The liquid water in the distribution channels is quantified at various operation conditions, e.g., temperature, inlet humidity, current density. This work attempted to generate quantitative data to establish a comprehensive understanding of the two-phase flow patterns in PEMFC gas channels. Taking advantage of direct high-resolution visualization with advanced image processing algorithms for extracting two-phase flow data in the gas channel, further quantitative studies have been done in PEMFC under different gas stoichiometric ratios, relative humidities, operating pressures, and temperatures. Information of total and local water coverage ratio at interested areas of a flow channel (elbows, middle region and each channel row) gave more insights into how flooded the flow channels are and also can be used for establishing the relationship between the water coverage and variations in the performance of a fuel cell.[44,57,58]

3.2. Two-Phase Transport in Membrane Electrode Assemblies (MEA)

The opacity of gas diffusion electrodes makes the visualization of transport within a porous electrode difficult. Liu and Pan performed a water breakthrough experiment through GDLs with or without a microporous layer (MPL) by simultaneous visualizing the generation of water droplets and measuring of the back pressure. It was found that in the GDLs the water began to breakthrough at some preferential locations and became continuous transports spots. It was also concluded that the morphology of GDLs can affect water discharge.[59] Kang et al. developed a similarity model experiment for indirect investigation of liquid water transport in hydrophobic GDLs.[60] Three dimensionless parameters of the model experiment, i.e., capillary number, viscosity ratio and bond number, were manipulated to simulate the practical operation of PEMFCs. The evolution of water distribution in the nonwetting material was photographed. However, the conditions were not necessarily the same as a real cell. The visualization under GDL surface remains as a challenge by conventional optical microscopy.

3.2.1. Fluorescence Microscopy

Fluorescence is a phenomenon that occurs when molecules absorb light with a certain wavelength (excitation), followed by a re-emission of light with a longer wavelength.[61] These excitation and emission wavelengths can be unique fingerprints of certain substances called fluorophores, which makes their use in sensing possible. It is a prospective approach to visualize the water transport in microscale under the surface of the GDL using fluorescence microscopy integrated with optical photography.

Lister et al. for the first time used fluorescence microscopy to characterize the time period of penetrating through gas diffusion media and also to understand the penetration pathways through the material for water.[62] A visualization experiment was conducted by feeding fluorescein dye though a GDL and correlating the light intensity to the height of the fluidic surface.

The images obtained from the visualization experiments were processed, which enabled the analyses of the connectivity among different flow paths and the interdependence of the liquid motion. Bazylak et al. from the same group explored the water transport behaviors on the surface and within the microstructure of the GDL by employing fluorescence microscopy and pressure drop measurements.[63] A changing breakthrough location of water droplet was observed, suggesting dynamic and interconnected flow paths of water within the GDL. This phenomenon was supported by an idealized numerical simulation, showing that once a new penetration pathway is formed, less preferable pathways recede. However, the time-dependant water transport within GDL has not yet been well studied.
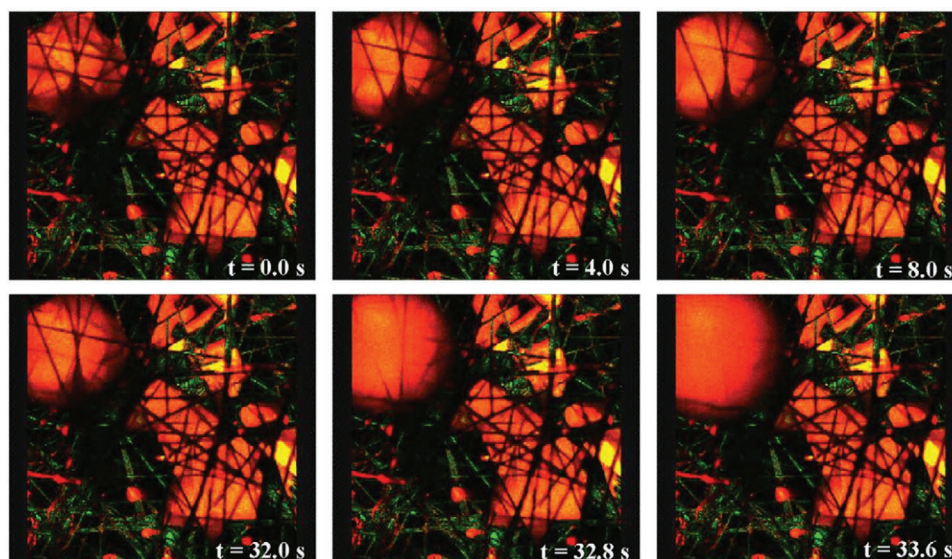
A laser-scanning confocal microscope technique was developed by Gao et al.[64] It was used to show the water transport behaviors in GDLs. In order to obtain visual images, water dyed with fluorescent Rhodamine B was forced to flow through different GDLs exposed under the confocal microscope. The pressure of water in the GDLs was monitored. Based on the pore-scale visualizations (**Figure 4**), they found that water flow in GDL of PEMFC was unstable and showed features of column flows in hydrophobic soils, which had been intensively studied with well-developed theories.[65] This study provided a guideline for the mathematical modeling of water transport and water management in PEMFCs.

Polytetrafluoroethylene (PTFE) based polymers are widely used as coating materials to form a hydrophobic surface on carbon fibers, as well as binder agents in fuel cell electrodes. Because there is lack of contrast between the carbon-based ink and carbon fiber in final images, uniform "black field" areas in the images has little or no observable features could be obtained through an optical microscopy. McCarthy et al. developed an approach using fluorescence microscopy to distinguish the location of PTFE/ Nafion in MEA and the gas diffusion media.[66] "Brilliant yellow 43" ($C_{20}H_{24}N_2O_2$) was used as a probe to track the distribution of PTFE within the GDL. It was found that the hot-pressing process which is used to fabricate membrane coated materials resulted in a physical dispersion of hydrophobic layers into the gas diffusion media itself. This was the first time to directly identify the distribution of PTFE in the gas diffusion layer.

3.2.2. Optical Fibers

Another approach used for opaque medium is to build optical waveguides. Of particular interest is optical fibers, which are cylindrical waveguides that could carry the optical signal confining within them. A most commonly used material in the fabrication of optical fibers is fused silica with a relatively high chemical inertness and thermal stability. Multiple configurations have been proposed using optical fibers as both active and passive medium. In active configurations, fibers will be coated with indicators suitable for fluorescence-, chemiluminescence-, or absorbance-based measurements, while in passive configurations, fibers are only used to carry light to and/or collect lights from the detection site.

Combined with fluorescence detection, Zhu et al. for the first time described a fiber-optic humidity sensor on the basis of a

**ADVANCED
SCIENCE NEWS**
www.advancedsciencenews.com

**ADVANCED
MATERIALS
TECHNOLOGIES**
www.advmattechnol.de

Figure 4. Visualization examples of wet GDLs with 1.5 mm × 1.5 mm field of view. Reproduced with permission.[64] Copyright 2009, Elsevier B.V.

Nafion membrane containing 1 wt% of Rhodamine 6G as an indicator.[67] The fluorescence intensity detected was attributed to the formation of a complex between immobilized Rhodamine 6G and water to quantify the humidity. The fluorescence intensity increased linearly with the partial pressure of water vapor. Based on Zhu's work, Yatin et al. made several improvements and developed a fluorescence fiber-optic setup to detect the change of water distribution inside a membrane of an operating fuel cell.[68] The setup is illustrated in **Figure 5**a. The measured results of water content in the membrane can be used to predict the dynamic response of fuel cells during various operating.

Hydrogen peroxide is a reactive species and an intermediate commonly formed during the operation of PEMFCs, which can accelerate the degradation of both the polymer backbone and the active ionic groups that are essential for ion conduction. Inspired by Yatin's work, a more sophisticated setup (shown in Figure 5b) to monitor the degradation of membrane in situ and ex situ was developed by Prabhakaran et al.[69] Cadavid et al. conducted a series of studies on fiber sensors to detect the presence and quantify the concentration of hydrogen peroxide.[70] The mechanism of H_2O_2 detection relies on the changes of absorbance of the metallic hexacyanoferrate compound, i.e., Prussian blue. With two early-stage ex situ trials on simply testing the concentration of H_2O_2 in solution and the effects of temperature on the intensity of reflected light, the authors were able to measure the concentration variation within the Nafion membrane.

3.3. Temperature Distribution

Infrared (IR) thermography is an optical method that has been widely used for measuring temperature distribution in PEMFCs. Hakenjos et al. conducted a very direct IR and digital observation of the electrode surface with a simultaneous measurement of current distribution.[48] It was found that the temperature distribution aligned with the current distribution

only in the areas without the presence of liquid water, indicating that water generation has a great influence on the local temperature. Taking advantage of IR thermography, Ishikawa et al. measured a PEMFC operating at temperatures below freezing point.[71] It was found that super-cooled liquid water can be generated at temperature as low as −10 °C. After several minutes' operation, the temperature increased to 0 °C while the water began to turn into ice. In a following work, Ishikawa developed a cross-section configuration (**Figure 6**) to further investigate the water behavior within the GDL at temperatures below freezing point.[72] During operation, the cell performance fell down with ice grew at the GDL/MEA interface.

Daino et al. carried out another in situ cross-section investigation to study the through-plane water transport in a PEMFC.[73] In order to obtain a view of the GDL cross-sections, the cathode and anode lands were recessed by 180 μm to represent the thickness of the GDLs used. Transparent material was used to form a window for the travel of visible. The observations revealed that water transport in the vapor phase was dominant in the anode GDL, while liquid water was routinely observed in the cathode GDL. It was found that the temperature gradient across the anode GDL is greater than the cathode GDL.

4. Optical Microscopy Studies of Lithium Batteries

Li-ion batteries have been regarded as a prevailing commercial leader for energy storage applications in the past decade. However, the performance still needs to be further increased to meet the increasing energy requirements in the future. To improve storage capacity and cycle life remains technical challenges that need further efforts. Several reviews have surveyed the development of different types of in situ and in-operando techniques for Li-ion batteries.[20,74] However, none of them gives a specific review on optical microscopy techniques. In this section, in situ optical microscopy for Li-ion batteries will be reviewed.
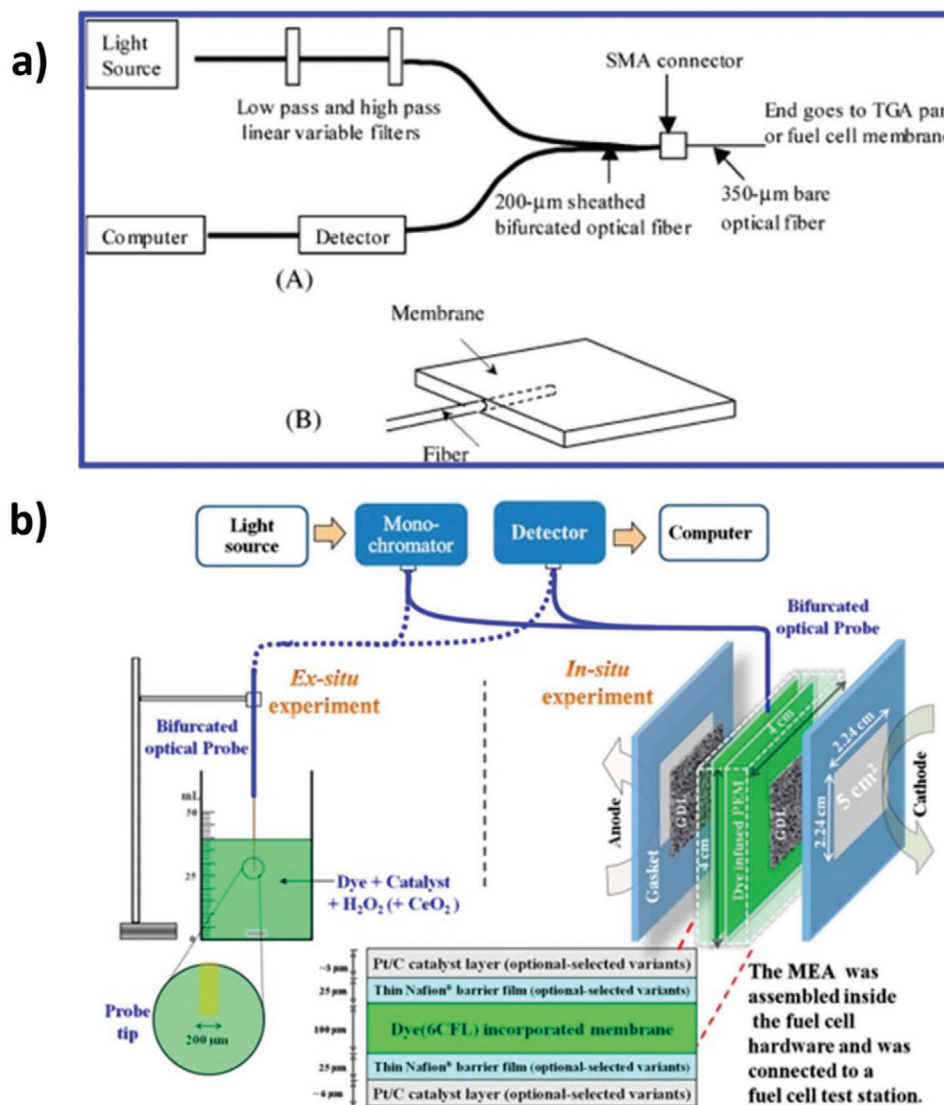
Figure 5. a,b) Schematic of two fiber-optic fluorescence instrument setups. a) Reproduced with permission.[68] Copyright 2005, American Chemical Society. b) Reproduced with permission.[69] Copyright 2012, National Academy of Sciences.

4.1. Observation of Morphology and Structure Evolution

4.1.1. Dendrites

Lithium metal is a promising negative electrode material which gives a high theoretical specific capacity. However, the widespread application of metallic lithium anode has been limited by challenges such as the nonuniform deposition of lithium during the charge-discharge cycles of the battery.[75] These deposits often present branch like morphologies referred as dendrites. Dendrites are actually commonly generated during electrodeposition of most metals, such as copper and iron. The dendritic morphology of electrodeposited lithium is related to the electrolyte compositions, surface morphologies, electrochemical conditions, etc.[76] The surface condition of lithium electrode is also known to play a critical role in the initiation of dendrites. It is also known that local variations of

solid-electrolyte interphase (SEI) composition and thickness will lead to an uneven current distribution and thus unsmooth deposition. With the growth of dendrites, the no uniform deposited film will crack and more lithium will be deposited near the cracks. Also, Li tends to deposit the regions where the film is thinner. It has been shown that lithium on the tips of dendrites is electrochemically inactive, decreasing the amount of available lithium.[77] However, this free lithium is extremely chemically active due to its large surface area. Dendrites can also traverse the separator and cause short circuit. The exact reason for the propensity of lithium to turn to dendritic morphology has not yet been confirmed.

Sano et al. conducted several studies for in situ morphological observation of lithium metal in lithium-ion batteries with ionic liquids as an electrolyte.[78–80] The experiments were performed with a house-made two-electrode cell containing a transparent window as shown in **Figure 7**. It was found that
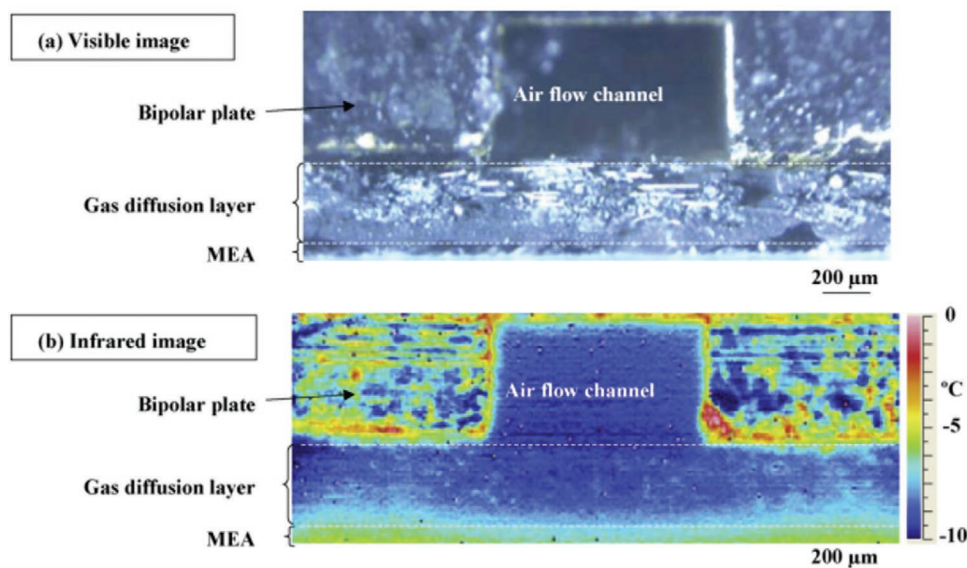
Figure 6. Cross-section inspection on PEMFC operating at a temperature below freezing point. Reproduced with permission.[72] Copyright 2008, Elsevier B.V.

the morphology of lithium electrode depended on current densities. Smaller-sized precipitation of lithium with higher coverage ratio was more likely to be obtained at larger current densities.[81] Lithium precipitation tended to grow at the places with pre-plated lithium. It was also observed that large potential drop was induced during the initial plating process. Nondendritic particle were obtained with additives of PP13[TFSA] and vinylene carbonate (VC), as a uniform film of decomposed VC was formed on the surface.

Steiger et al. fabricated a planar cell to study the deposition and dissolution of electrodeposited lithium.[82–84] Lithium was deposited as filaments. Those wires grew from the interface between the current collector and lithium metal. A simple and effective method with a capillary cell to explore the growing mechanism of lithium dendritic was developed by Bazant et al.[85] The setup is show in Figure 7a. The authors suggested two mechanisms for lithium growth. Moss like lithium growth from the roots dominated the morphology when the battery was below the Sand's capacity. On the contrary, if the battery was operated above the Sand's capacity, dendritic lithium grew,

which could penetrate the separator and cause a short circuit. Therefore, increasing the salt concentration in electrolyte to maximizing the Sand's capacity can avoid the formation of dendritic lithium.

Aryanfar et al. developed a method for quantitative determination of the amount of dead lithium crystals in a coin cell.[86] The specially designed cell was comprised of an acrylic separator sandwiched by two current collectors as shown in **Figure 8**b. The transparent acrylic structure provided a light path for visualizing dendrite growth. With digital imaging, they recognized two different types of micro morphology: dead lithium crystals and dendrites. They further studied the thermal annealing kinetics of lithium dendrites by both experiments and simulations with same structure.[87]

The mechanistic study of battery failure using in situ characterization techniques is still challenging. Most of previous studies focused on half-cells with lithium as negative electrodes. The operating conditions are not necessarily the same as or close to commercial cells. Guo et al. designed an all-quartz glass full cell for in situ monitoring of electrodes occurring
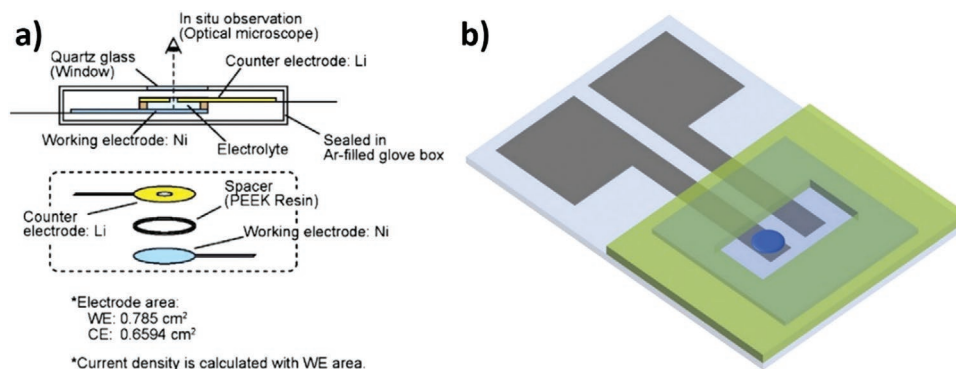
Figure 7. Two custom-made two-electrode half-cell with transparent window for optical observation: a) Coin cell. Reproduced with permission.[78] Copyright 2010, Elsevier B.V. b) Planar cell. Reproduced with permission.[82] Copyright 2014, Elsevier B.V.
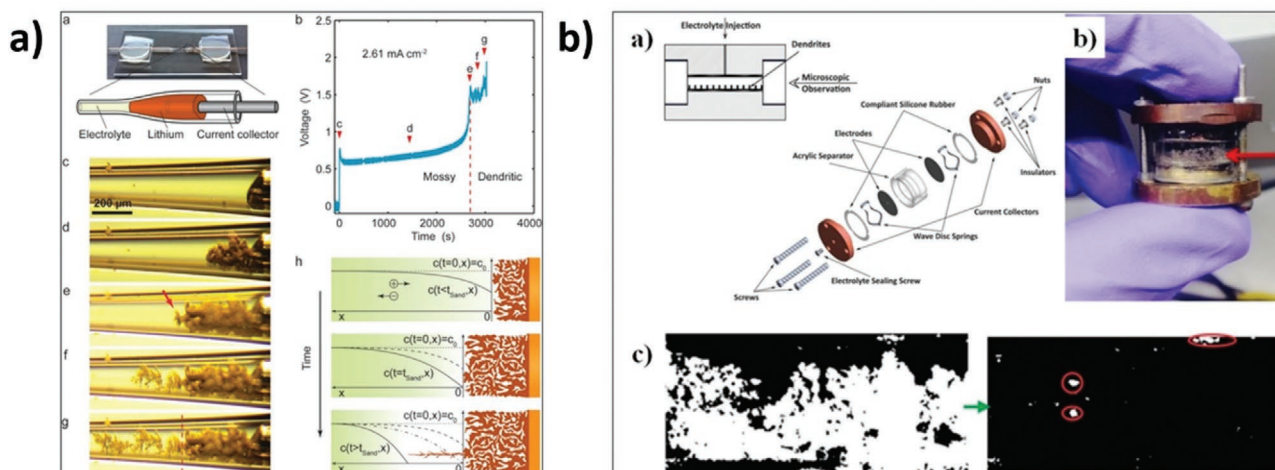
Figure 8. Transparent a) capillary and b) coin cell structure for dendrite observation. a) Reproduced with permission.[85] Copyright 2016, The Royal Society of Chemistry. b) Top: Reproduced with permission.[86] Copyright 2014, Royal Society of Chemistry. Bottom: Reproduced with permission.[87] Copyright 2015, AIP Publishing.

during charging/discharging cycles.[19,88] In order to record of internal phenomena in real time, the anode and cathode were designed side-by-side as shown in **Figure 9**. In a face-to-face in operando cell configuration, Mukherjee et al. investigated the effects of high C-rate on the lithium plating on graphite electrode.[89] Irreversible lithium plating lowered the anode potential, which leads to rapid performance degradation.

Ding et al studied lithium dendrite formation based on a cell with a glass window and developed an understanding of the effects of various electrolytes.[90] Moreover, metal contamination on electrode is a serious problem which leads to short circuit and declination of the cell performance. Kuwabara and Sato conducted real time observation on the cross-section of battery to detect how contaminations like copper attached on the electrode in a charging process, using an confocal microscope.[91]

4.1.2. Electrode Volume Change

In addition to lithium, materials such as silicon and tin can be attractive for negative electrodes of lithium-ion batteries. The reaction of lithium with these materials is alloying process. During reaction, new intermetallic phases will form, which normally have different crystal structures and larger crystal volume compared to the original one. This is believed to be a main reason of cracking and loss of electrical contact.[92] In some cases, the
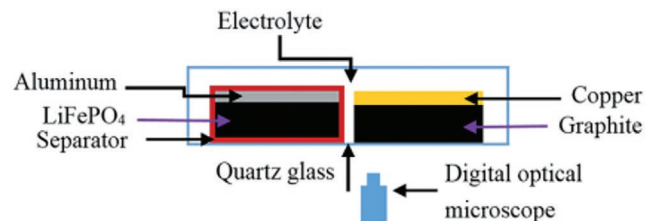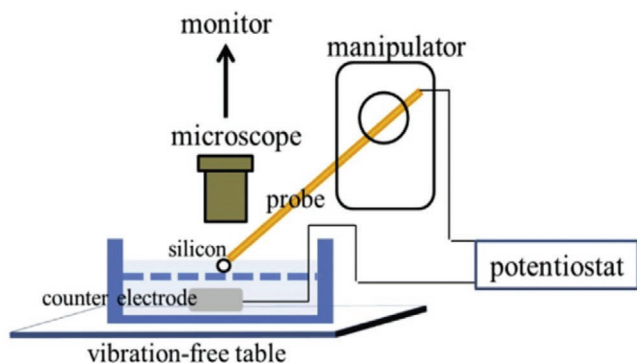
cracking of electrode particles can be minimized if the volume change is homogeneous on optimized particles.[93] It is essential to study and monitor such volume changes of these materials.

Beaulieu et al. conducted several investigations to study the morphology change of electrode materials during the reaction with lithium by using atomic force microscopy and an optical CCD camera.[94,95] The cell was designed as a glass chamber with a glass cover-plate. Through this design, the morphology and volumetric change during operation cycles were observed. Timmons et al., from the same group, made a direct observation of the particle of amorphous active materials. Upon lithium insertion, the particles expanded isotropically with a large volume change,[96] indicating a better durability during cycling.

Kanamura's group introduced a single particle measurement technique for in situ study of the volume expansion behavior of a secondary particle of different materials, including graphite, $LiCoO_2$, $LiFePO_4$ and silicon (**Figure 10**).[97–101] The setup can function properly as a battery and its electrochemical performance of different electrode materials can be evaluated in electrolytes. With this system, they observed that the apparent volume expansion of one silicon secondary particle was larger than the theoretical expectation. A possible reason was that the silicon secondary particles used in their study were aggregated by several primary particles with smaller size, which resulted in an anisotropic property.

4.1.3. Stress Evolution

In lithium electrodes with large capacities, enormous strain can be caused by the incorporation of interstitial lithium atoms. The induced stress and strain are responsible for most mechanical damage of electrodes. For example, silicon could experience volume expansion of more than three times upon complete lithiation, which would lead to a generation of remarkable stresses as high as 1–2 GPa.[102] The mechanical damage will directly result in capacity loss and battery failure. In order to establish a mechanistic understanding of such damage, the measurements of essential mechanical properties of electrode are important.

Figure 9. All-quartz transparent cell with electrodes placed side-by-side. Reproduced with permission.[88] Copyright 2015, Royal Society of Chemistry.

ADVANCED
SCIENCE NEWS
www.advancedsciencenews.com

ADVANCED
MATERIALS
TECHNOLOGIES
www.advmattechnol.de

Figure 10. Schematic illustration of the single particle measurement technique setup, which composes of a Li metal counter electrode and a Pt microwire sealed in glass capillary. This wire works as current collector by attaching single particles dispersed on a glass-fiber sheet for electrochemical testing. Reproduced with permission.[97] Copyright 2013, Elsevier B.V.

Many studies have been reported to investigate the stress evolution within electrodes. Cantilever beam-deflection method is a widely used optical inspection technique. By detecting the shift of reflected laser beam from the object surface, the curvature of the material can be calculated.[103] However, this technique is very vibration sensitive and severe errors and noise in stress measurement can be generated. Sethuraman et al. presented a series of experimental efforts to measure the stress evolution and the biaxial modulus change of silicon thin-film electrode along with lithium concentration.[104–106] Stress in the silicon film was measured using a multibeam optical sensor wafer curvature system (k-Space Associates, Dexter, MI) by detecting the substrate curvature changes, as shown in **Figure 11**. In this system, a transparent window was designed in front of the cantilever allowing the deflection of light beams.
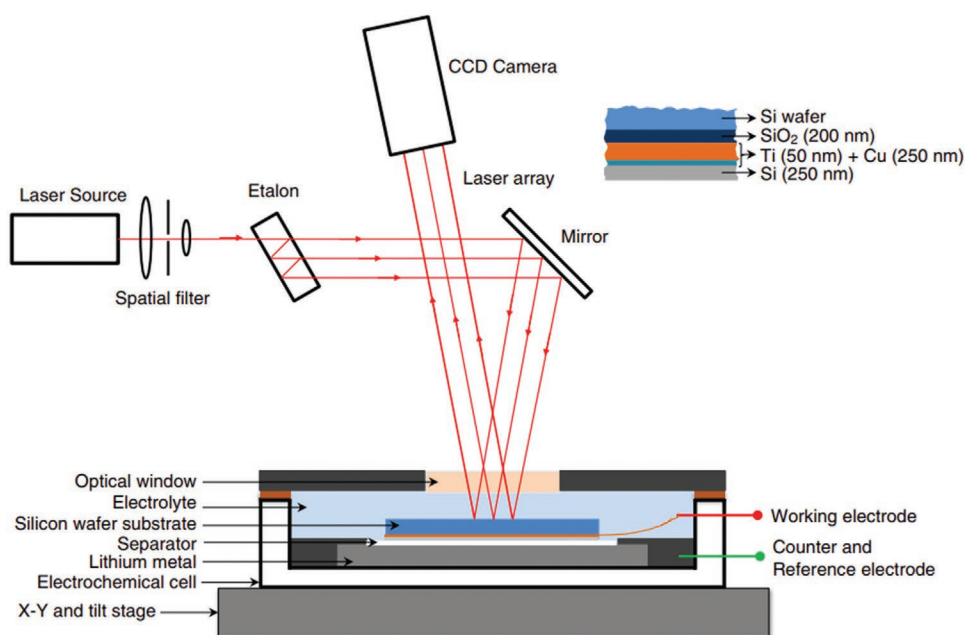
With a similar setup, Sethuraman et al. further made real-time stress measurements on composite graphite and germanium electrodes in a lithium-ion cell. The stress developed during cycling in graphite is significantly smaller than that in silicon electrodes (max. 10–12 MPa).[107] For germanium thin film electrodes,[108] it was found that upon lithiation, germanium electrode underwent extensive plastic deformation, the measured compressive stress could be as high as 0.76 GPa. Unlike silicon or tin, LiTiO showed negligible strain upon electrochemical cycling (<0.2% volume change). In order to investigate the stress evolution of this material, Choi et al. developed a very sensitive measurement technique based on a laser in situ substrate curvature setup (**Figure 12**).[109] Increasing the accuracy of the spot position to confine it within 200 nm was shown to extend the determination of curvature to up to 60 km.

Pharr et al. developed an electrochemical cell to conduct quantitative measurements of fracture energy of a silicon electrode at different status as shown in **Figure 13**.[110] The cell was fabricated with hermetic Teflon with a glass window for morphology monitoring by optical microscopy and strain measurement by multibeam optical sensor. In a following study, Pharr conducted further experiments to provide insights into the plasticity of Li_xSi thin films.[111] From the results of these experiments, the fracture energy was calculated as a function of lithium concentration based on a fracture models.[112] Pharr et al. also performed an in situ measurements of stresses, stiffness and fracture energy of a-Li_xGe electrodes during charging/discharging operations.[113]

V_2O_5 has also been regarded as an alternative cathode material for lithium-ion battery. In order to obtain the dynamic strain fields of V_2O_5, Chen et al. built an electrolytic cell equipped with a quartz, in which V_2O_5 nanobelt and lithium foil were fixed on one end by two holders as working and counter electrodes, respectively.[114]

Figure 11. A multibeam optical sensor wafer curvature system for strain measurement in lithium-ion battery. Reproduced with permission.[104] Copyright 2010, Elsevier B.V.

ADVANCED
SCIENCE NEWS
www.advancedsciencenews.com

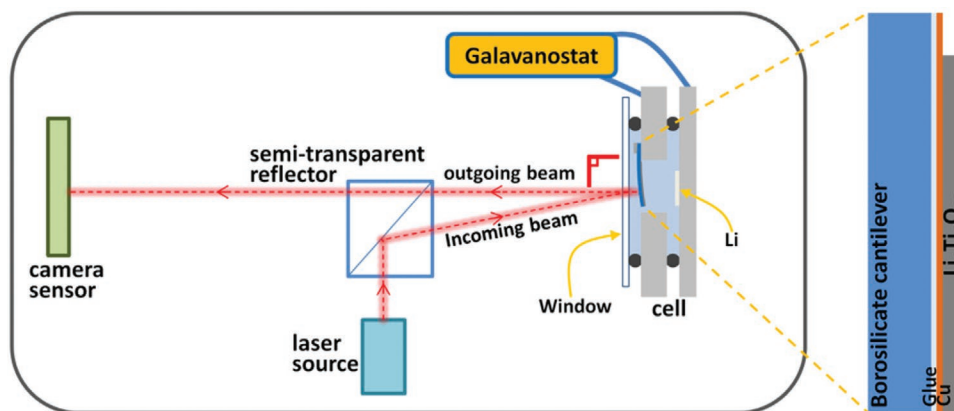ADVANCED
MATERIALS
TECHNOLOGIES
www.advmattechnol.de

Figure 12. Sensitive measure setup based on a laser in situ substrate curvature. Reproduced with permission.[109] Copyright 2013, Elsevier B.V.

4.2. Species Distribution

4.2.1. Colorimetric Methods

The color changes of materials during electrochemical reactions can also be harnessed to indicate the state change within a battery cell. Some intercalation materials such as graphite experience a color change upon electrochemical insertion of lithium. Specifically, lithium can form various ordered stages when reacting with graphite. These stages show their own distinct colors. Therefore, optical microscopy can be directly used to visualize the lithiated states in graphite. Uhlmann et al conducted a systematic calibration to correlate different colors of graphite with different states of charge (SOC).[115] Graphite was found to

R. E. - reference electrode C. E. - counter electrode. W. E. - working electrode

Figure 13. A multibeam optical sensor wafer curvature system for strain measurement of multi electrodes. The cell employs lithium as both reference and counter electrode, and an array of silicon working electrodes. At various stages of delithiation, the electrodes were disconnected one by one from the cell such that they were only partially delithiated. Reproduced with permission.[10] Copyright 2013, American Chemical Society.

changes its color from black, via red, to gold depending on the SOC (shown in **Figure 14**).

Taking advantage of colorimetrics, Maire et al. developed an approach to investigate the lithium mobility in composite graphite electrodes.[116,117] As shown in **Figure 15**, a specially designed cell with a glass window was constructed to perform the studies by heterogeneously charging. A correlation between RGB color values and lithium contents was established. The SOC can then be calculated from the RGB values of each pixel in a photograph. By observing the movement of the diffusion front and the state of graphite, the diffusion coefficients and activation energy were calculated. Harris et al. conducted a similar experiment to observe the lithium transport in an operating cell.[118]

Thomas-Alyea et al. presented in situ optical images showing that there is considerable spatial nonuniform distribution of lithium in a graphite electrode on the microscale during charging/discharging cycles.[119] When the graphite electrode began to be lithiated, the nucleation of golden regions was clearly seen at the particle edges, while there was no color change in the interior regions. If lithiation continues, the golden phase front moved from the edges into the interior. During delithiation, when the cell was at an intermediate SOC, interior regions of the particles were still remain golden, while the exterior region turned to red.

Bhattacharya et al. observed the degradation of graphite surface during electrochemical cycling, through constructing a cell with a quartz glass optical window.[120] Electrode degradation was observed during the lithiation and de-lithiation processes. Tatsumisago et al. conducted an optical inspection on graphite composite electrodes in all-solid-state lithium batteries to monitor the color changes.[121] The color changes enable researchers to evaluate reaction distributions in graphite electrodes. With a mixing ratio of 50:50 of graphite particles and glass particles ($75\%Li_2S \cdot 25\%P_2S_5$), graphite within the electrode changed to gold color, suggesting that all graphite particles were fully lithiated.

Optically monitoring experiments on color change were mostly performed on graphite anodes. Amorphous silicon has also been found experiencing a color evolution during lithiation/delithiation cycle.[122] Different from graphite, the color evolution depends on electrode thickness and compositions
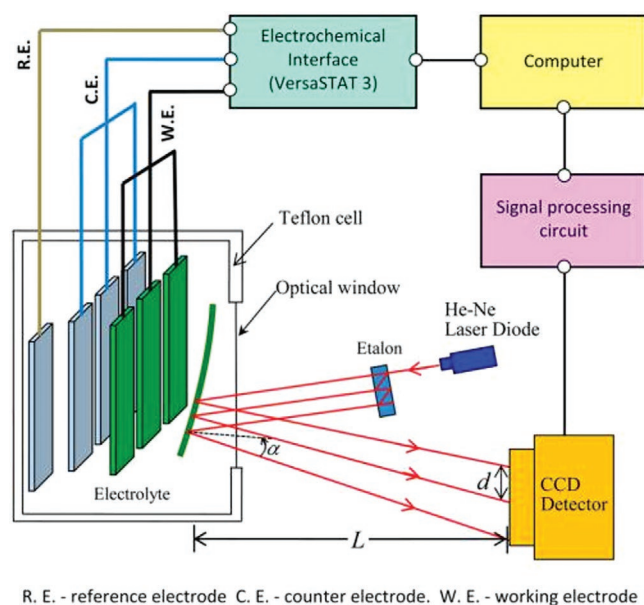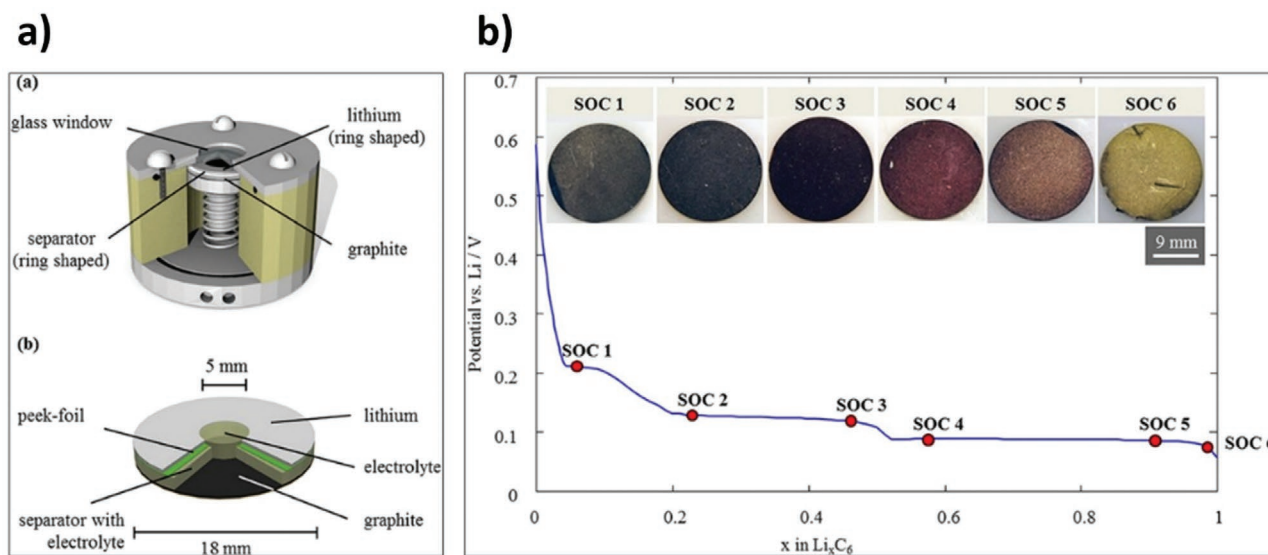
**ADVANCED
SCIENCE NEWS**
www.advancedsciencenews.com

**ADVANCED
MATERIALS
TECHNOLOGIES**
www.advmattechnol.de

Figure 14. Setup for graphite optical observation and the color of graphite at different SOC. Reproduced with permission.[115] Copyright 2015, Elsevier B.V.

within the system. Cathode materials, such as lithium iron phosphate with lower conductivity, are difficult to be observed because of the high light absorption of the carbon additives that are used to improve the conductivity of electrodes. Rosher and Riemschneider modified the cathode composites by replacing carbon with indium tin oxide (ITO) to improve the optical accessibility and maintain the conductivity.[123] Using the modified electrodes, a reproducible and reversible change in optical reflectance and color from a home-made transparent cell during cycling can be visible and recorded, which could indicate the state of charge of the electrode.

Optical transmittances of a crystal MoS_2 were found as a function of lithiated states and electrochemical potential by Wang et al. They built a planar battery for in situ transmittance measurement during lithiation of MoS_2 as illustrated in **Figure 16**a).[124] In Figure 16b), MoS_2 was observed under the illuminating light with 450 nm wavelength. Its transmittance was found to increase by decreasing potentials from 2.8, 0.9 to 0.05 V (vs Li^+/Li). Under TEM and AFM, the formation of an interconnected Mo nanoparticle network was observed in the thick MoS_2 crystals after rapid lithiation, which enabled an

increase in electrical conductivity compared to pristine MoS_2. Another observation on MoS_2 was conducted by Itaya et al. Their study, for the first time, obtained the images of dynamic intercalation of Li into MoS_2 single-crystal electrodes.[125]
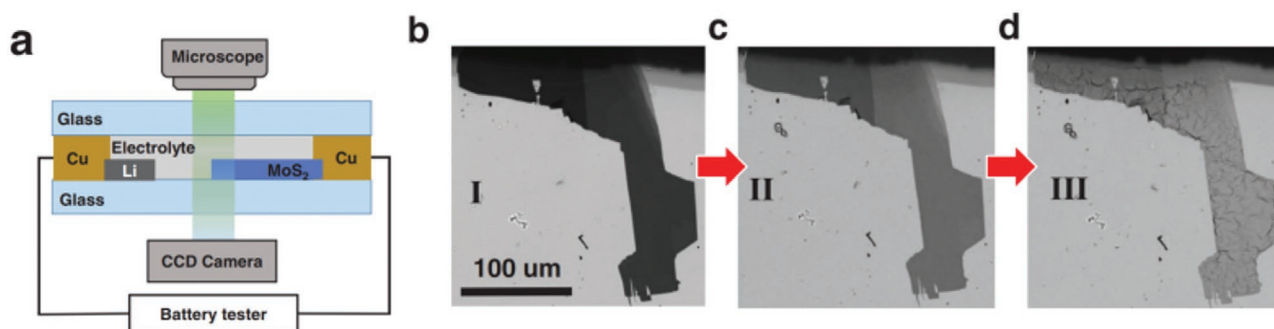
4.2.2. Addition of Tracers

Fluorescence-based imaging provides opportunities to visualize trace amounts of ions with an ultrahigh resolution. However, the complex environment has limited the use of fluorescence imaging in batteries. In 2015, Yu et al. for the first time employed an X-ray fluorescence microscopy to monitor the morphology change in a Li–S battery[126] In their study, the morphology change of the sulfur electrode and redistribution of sulfur and polysulfides were monitored in real time.

Sun et al. explored the formation of the polysulfide species from a sulfur electrode and their diffusion in the electrolyte of a Li–S cell with a direct visualization design.[127] As shown in **Figure 17**, the cell consisted of a small glass pipette for housing an electrolyte, two stainless steel bolts as current collectors and
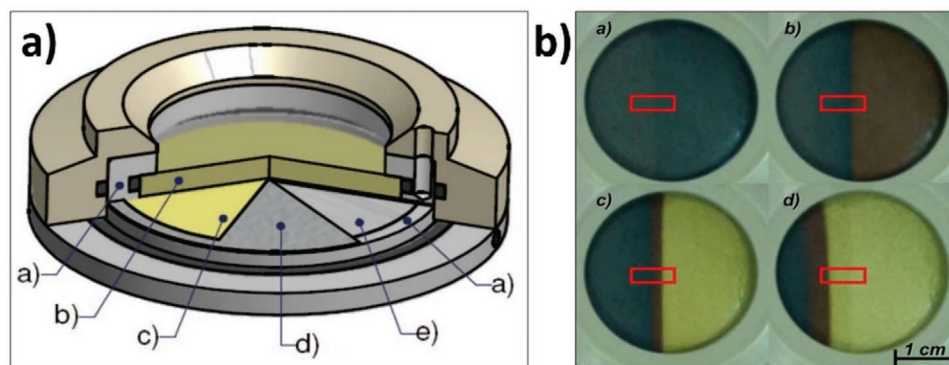
Figure 15. a) Schematic illustration of the transparent cell with glass window for kinetic studies using colorimetry. b) RGB images taken at a) 0 h, b) 11 h, c) 26 h, and d) 110 h during charging. Reproduced with permission.[117] Copyright 2009, Elsevier B.V.

ADVANCED
SCIENCE NEWS
www.advancedsciencenews.com

ADVANCED
MATERIALS
TECHNOLOGIES
www.advmattechnol.de

Figure 16. a) Schematic of the microbattery for in situ transmittance measurement of MoS_2 electrode and b–d) the optical images of a MoS_2 flake under different status of lithiation. Reproduced with permission.[124] Copyright 2014, WILEY-VCH Verlag GmbH & Co.

mechanical supports for a sulfur cathode and a lithium anode. The experiment revealed detailed processes of electrochemical degradation in a lithium–sulfur battery. During cycling, dissolution of sulfur-based composite can be observed via the changes of the color of the electrolyte. The changes of colors transformed consistently with the electrochemical profiles, showing the distribution of polysulfides over the discharge process.

$LiNi_{0.5}Mn_{1.5}O_4$ cathode in Li-ion batteries experiences complicated interfacial interactions with electrolytes during charge/discharge cycles. A protective film will be generated on the electrode surface which can extend battery life. Meanwhile, Ni and Mn dissolve into the electrolyte, which can cause a drop of performance of a battery. Using optical fluorescence spectroscopy, Jarry et al. identified the formation of several fluorescent Ni_{II} and $Mn_{II/III}$ complexes on the graphite electrode from a tested $LiNi_{0.5}Mn_{1.5}O_4$/graphite coin cell after 600 cycles.[128] Based on the result, they proposed possible reaction pathways at the surface between $LiNi_{0.5}Mn_{1.5}O_4$ and organic carbonate electrolytes. After that, Qiao et al. directly visualized the dissolution of Mn^{2+} from $LiMn_2O_4$ by fluorescence imaging as shown in **Figure 18**.[129] The temporal and spatial distribution of Mn^{2+}

($<10 \times 10^{-6}$ M) was visualized, which provided fundamental understanding of the processes in battery systems.

One of the reasons behind battery degradation is the presence of trace water. Ren et al. studied the trace water in Li-ion batteries using fluorescence spectroscopy.[130] They developed a platform using nanosized coordination polymers for the detection of water molecules. In 2017, Padilla et al. for the first time tracked lithium ions in a battery electrolyte using widefield fluorescence microscopy.[131] By using 2-(2-hydroxyphenyl)-naphthoxazole as an indicator of lithium ions, they provided spatial and temporal distribution of lithium ions in a battery cell.

5. Optical Microscopy Studies of Redox Flow Batteries

Redox flow batteries (RFBs) are energy storage devices relying on reversible oxidation and reduction of redox couples dissolved in electrolytes. RFBs are particularly suitable for large-scale energy storage. The performance of RFBs is sensitive to
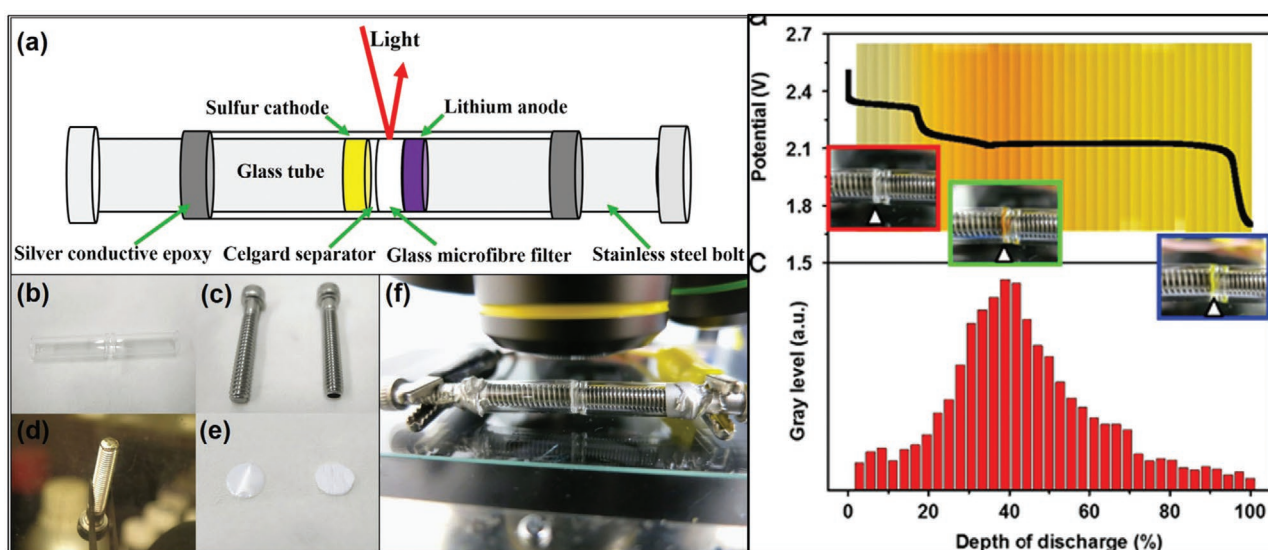
Figure 17. Schematic illustration of glass pipette cell structure for electrolyte color monitoring in lithium–sulfur battery. Reproduced with permission.[127] Copyright 2014, Elsevier Ltd.
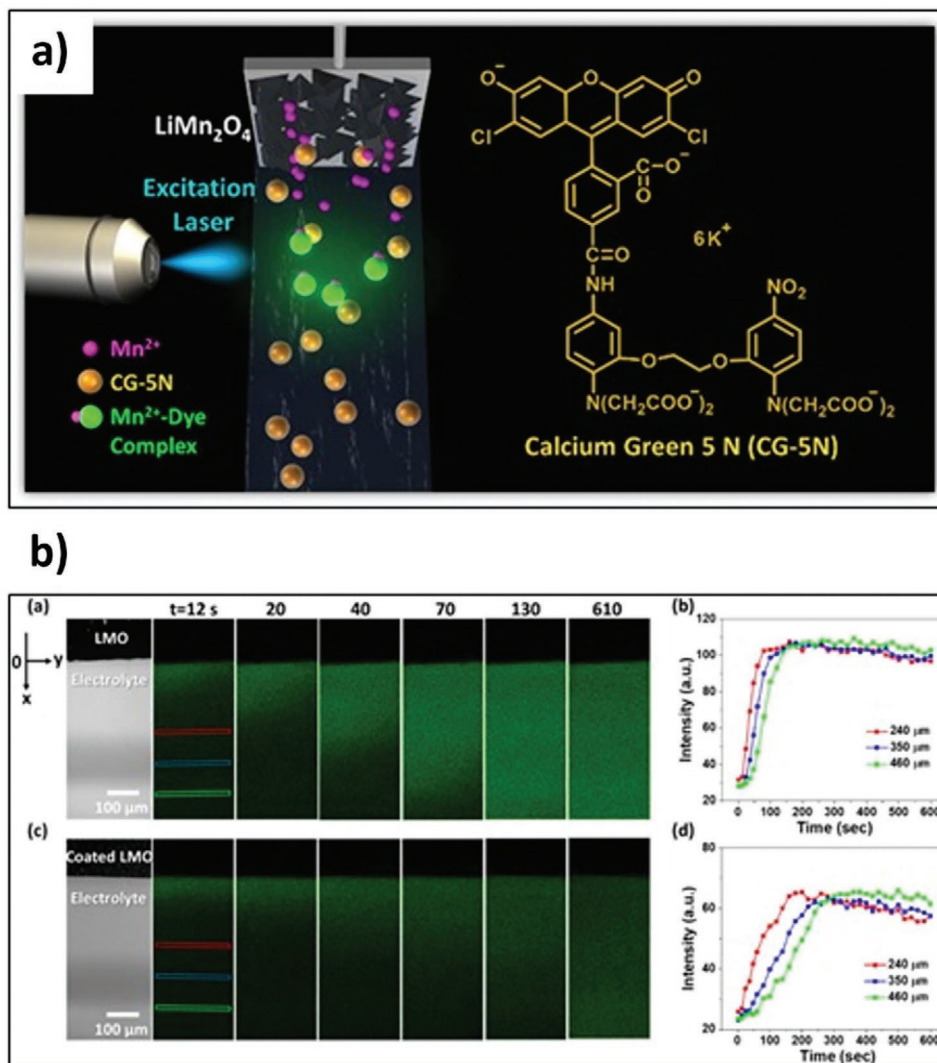
Figure 18. a) Scheme of the setup to visualize Mn^{2+} ion diffusion in battery systems by fluorescence microscopy and b) fluorescence images of diffusion of Mn^{2+} and the intensities at different positions over time. Reproduced with permission.[129] Copyright 2017, Elsevier Ltd.

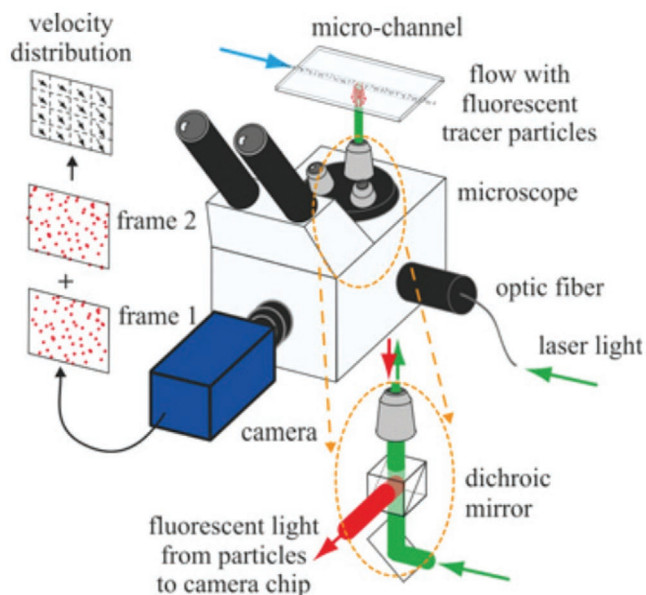the electrolyte flows. Several studies have been reported to visualize the transport processes in RFBs.

Houser et al. visualized the electrolyte distribution in an all-vanadium redox flow batteries by using a thermally responsive layer.[132] A window was designed on a customized end plate to allow the visualization of both mass and heat transfer. Wong et al. utilized fluorescence microscopy to study the reactant transport in the electrode microstructure.[133,134]

In order to study the flow filed in the flow channels, micro-particle image velocimetry (PIV) was implemented. In a study by Martin et al., the authors introduced PIV to measure the flow field within the channels.[135] A more sophisticated PIV measurement was presented by Brugmann et al as shown in **Figure 19**.[136] In Brugmann's work, the spatial and temporal velocity distribution of the electrolyte upon the formation and movement of gas bubbles and slugs in the channel were well measured. It provided a deeper understanding of the coherence of fluid motion in the channel and the electrochemical performance of cells.

Rubio et al. presented a method based on electro-chemiluminescent reactions to optically observe the mass transfer in liquid electrolytes.[137] The apparatus configuration is shown in **Figure 20**. The study used luminol as a probe molecule. In the observations, dead-end regions, which block the reaction sites of electrode, were seen. The results also demonstrated that in a flow battery with porous electrodes, bypass of electrolyte happens.

6. Optical Microscopy Studies of Zinc Ion Batteries

Zinc-based batteries are promising candidates for future energy storage considering its advantages such as low toxicity, abundance and high energy density. While Zn batteries have been widely used as primary batteries for many applications, the development of rechargeable Zn batteries are facing many challenges. One of the major issues is the formation of dendritic

**ADVANCED
SCIENCE NEWS**

www.advancedsciencenews.com

**ADVANCED
MATERIALS
TECHNOLOGIES**

www.advmattechnol.de

Figure 19. Schematic graph and the working principle of microparticle image velocimetry for measurement in microchannels of RFBs. Reproduced with permission.[136] Copyright 2012, Elsevier Ltd.

Zn, especially during high-rate charging, which can cause safety problems and shorten battery life.

Similar to lithium-ion batteries, the dendrite observation was conducted in half cells or specially designed full cells with optical windows. With real-time observation of the dendrite growth, the morphology evolution during Zn electrodeposition in Zn-ion battery was investigated and characterized.[138] The effects of deposition current/voltage[139,140] and solution conditions,[141] on the generation of dendrites were studied. Live tracking of Zn dendrite growth under optical microscopy was also employed to study the suppression of Zn electrodeposition by adding additives in the electrolyte.[142] A quick propagation of Zn dendrite happened within 30 min (from t_0 to t_3 in

Figure 21 left). By adding higher concentrations of polyethylenimine as suppression additive in the electrolyte, suppression of the growth of Zn dendrite could be clearly seen in the Figure 21 (right).
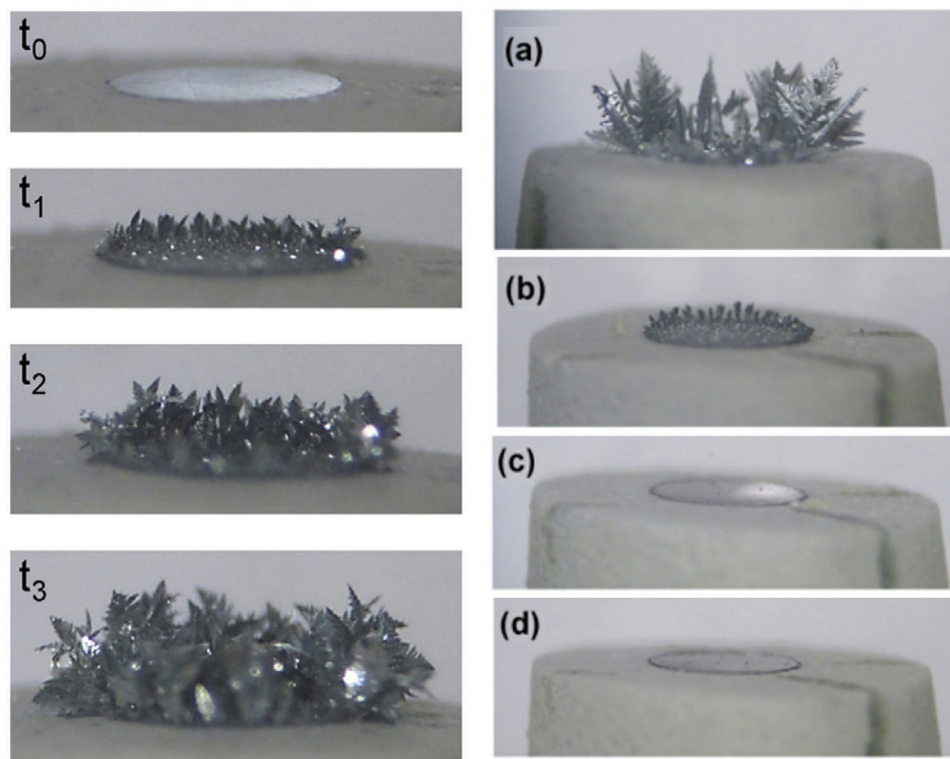
7. Future Perspectives

Optical microscopy has been prominently developed since its appearance. Its applications have been largely extended with higher resolutions and the development of new types of microscopes. The digitalization of pictures together with the powerful processing capability of modern computers allow for incredibly sophisticated analyses. Most optical microscope techniques were initially designed for applications in biology. With the development of EES, optical microscopy has significantly contributed to add values to the existing scientific knowledge. With its advantages of simple operation, high resolution, and nondestructive nature, it is the easiest technique to access and operate for in situ/operando studies. However, the applications of optical microscopy are limited to the surface study due to the lack of ability to penetrate opaque substances. This has driven the use of fluorescence microscopy and fiber-optic detection. Disregarding the significant progresses achieved, the opacity nature of most system components is still a barrier for using optical microscopy to study the processes inside EESs, especially within the solid-state batteries and for different interface problems between solid, liquid and gas. In the meantime, the inherent limits of resolution determined by the wavelength of light prevent research from going below nanometer scale. These challenges might be addressed with future development of transparent conductors and super resolution microscopy.

7.1. Transparent Conductors

The development of transparent conductors such as indium tin oxide (ITO),[143] conductive polymers,[144] and ultrathin 2D
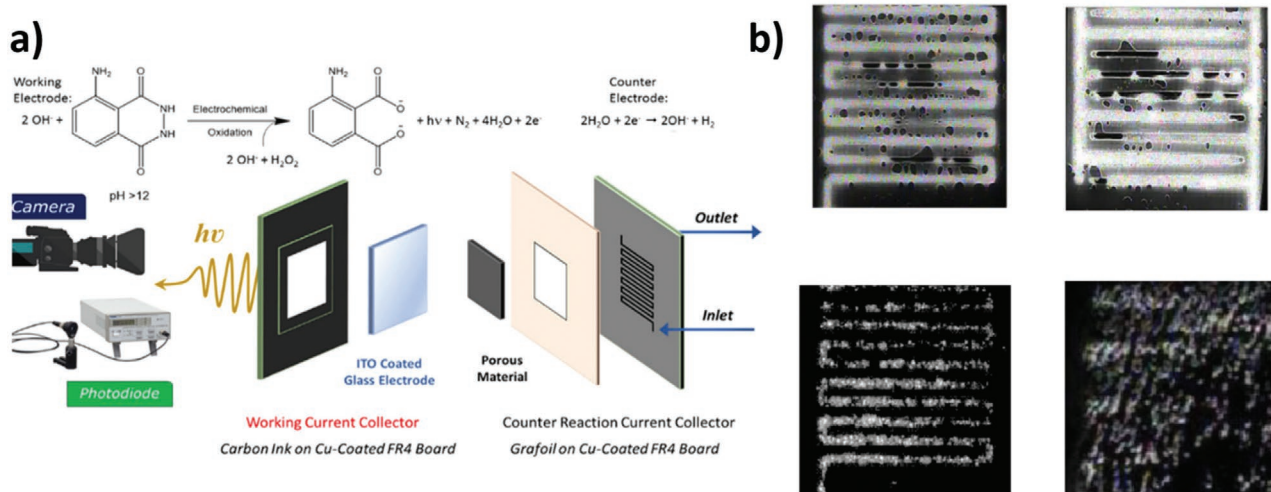
Figure 20. a) Explosive view of setup for mass transport visualization based on electro chemiluminescent reaction, b) showing the effect of flow field. Reproduced with permission.[137] Copyright 2018, Elsevier.

**ADVANCED
SCIENCE NEWS**
www.advancedsciencenews.com

**ADVANCED
MATERIALS
TECHNOLOGIES**
www.advmattechnol.de

Figure 21. Live tracking of Zn dendrite evolution using optical microscopy (left) at different time without additive; with different concentrations of polyethylenimine additive (right): a) 0 ppm, b) 10 ppm, c) 50 ppm, and d) 100 ppm, after electrodeposition for 30 min. Reproduced with permission.[142] Copyright 2014, Elsevier Ltd.

material[145] provides new opportunities for designing new in situ/operando electrochemical devices.

Of different transparent conductors, ITO has been most widely used to fabricate transparent conductive films due to its advantages of low resistance and high transmittance for visible light. However, practical applications of ITO are limited by its poor chemical stability under harsh conditions.[146] Ultrathin 2D materials such as TiO_2 and graphene are becoming attractive for transparent conductor applications due to their impressive optical transparency and outstanding conductivity,[147] which can be comparable to ITO films. A sheet resistance of 30 Ω sq^{-1} and an transmittance of over 97% for visible light have been achieved on single-layer graphene.[148] Nevertheless, it is difficult to prepare large-area graphene films without defects by either chemical vapor deposition or reduced graphene oxides (RGO), which makes the practical application of graphene-based transparent conductors challenging.[149] The high price of transparent electrodes made by chemical vapor deposition further restricts them to replace ITO. By contrast, RGO with lower costs has successfully been employed in several electronic applications including supercapacitors and solar cells.[150]

Transparent conductors have been used for optoelectronic devices and electrochromic devices over the last decade. Despite significant scientific progress, the practical applications of transparent conductor are at their early stage. Further applications in the electrochemical field can potentially be made, as either current collector or electrode materials, to design in situ/operando electrochemical cells. Hu et al. developed a printed graphene oxide network for sodium-ion intercalation. With an expanded interlayer distance, the RGO allowed sodium-ion intercalation. When the RGO was fully filled with sodium, the transmittance increased from 36% to 79% (**Figure 22**). Also, a large decrease of sheet resistance from 83 k to 311 Ω sq^{-1} was observed, showing the best electrical performance as a RGO-based transparent electrode.[147]

7.2. Single-Molecule Super-Resolution Imaging

The conventional optical microscopy is restricted by its spatial resolution. With the advances in detectors coupled with dye technologies and image processing methods, the optical limitation can be overcome using single-molecule fluorescence microscope (SMFM). It represents a subset of fluorescence microscopes (e.g., Total Internal Reflection Fluorescence microscope, Photoactivated Localization microscope and Stochastic Optical Resolution microscope) which use fluorophores to tag and detect single molecules.[151] SMFM was initially proposed to study the catalysis of single enzyme molecules.[152–154] It was then widely employed to investigate heterogeneous chemical catalytic activities of layered hydroxide microcrystals,[155] metal oxide semiconductors[156] and metal nanoparticles.[157,158] New studies with more powerful SMFM continue to emerge.
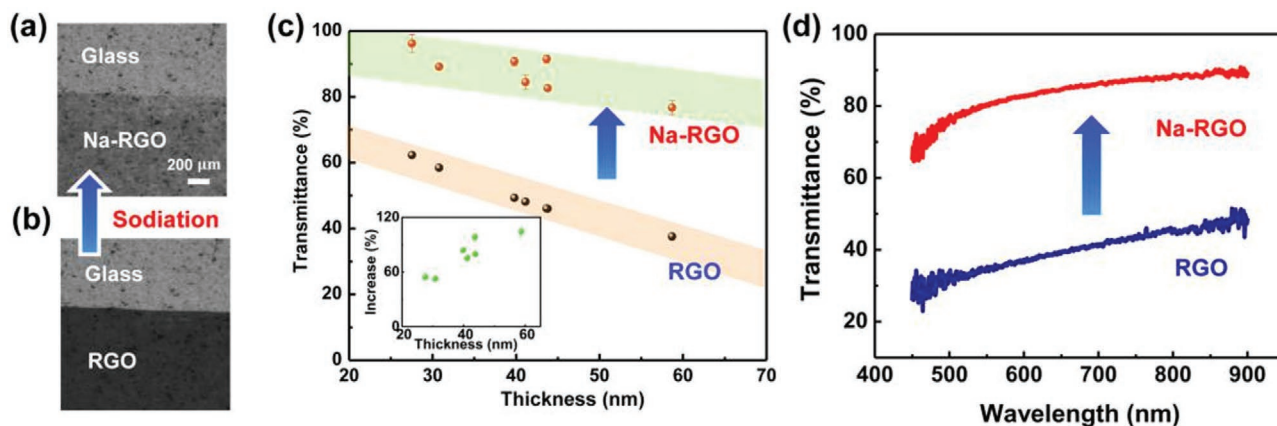
Figure 22. Change of optical transmittance of reduced graphene oxides films before/after solution–ion insertion (sodiation). a,b) Images (transmittance mode) of an RGO film before/after sodiation. c) Transmittance of RGO films with different thickness before/after sodiation under light with wavelength of 550 nm. d) Transmittance of an RGO film before/after sodiation under lights with wavelength from 450 to 900 nm. Reproduced with permission.[147] Copyright 2015, American Chemical Society.

Using a wide field total internal reflection fluorescence microscopy, Xu et al conducted several studies, achieving both super spatial and temporal resolutions. It allowed for investigations of the catalytic dynamics of nanoparticle catalysts within a single turnover.[159–162] It has been a challenge to characterize the heterogeneous catalytic activity on single particle due to the small structural scale, ubiquitous heterogeneity among particles and the fleeting time scale of the catalytic reaction. SMFM is a powerful tool to investigate and understand the catalytic behaviors of single nanoparticles with a high spatiotemporal resolution. Significant heterogeneous catalytic activities were observed at different surface sites on the nanoparticles. For nanorods and nanoplates, the ends generally had higher catalytic reactivity with more amount of low-coordination sites than their side facets.[163,164] Several recent reviews covered the studies on single molecule microscopy in the applications of chemistry, biology and life science.[165,166]

These works can shed light on old problems in electrochemical areas, such as the low oxygen reduction reaction and oxygen evolution reaction catalytic activity of nonprecious metal and lithium ion transport dynamics in nanoscale in the battery.

8. Conclusions

In this review, in situ/operando optical microscopy for probing electrochemical energy systems are discussed. Techniques together with corresponding methodologies and setup designs are highlighted. Overall, optical microscopy is a powerful tool for studying electrochemical systems. Limitations and future directions are also discussed. One of the critical challenges would be the design of in situ electrochemical cells that have a close environment with practical cell models and provide access for transmittance light at the same time. With the capabilities of directly visualizing and post processing of digital images, optical microscopy will continue to be a powerful tool for understanding and developing advanced EESs.

Conflict of Interest

The authors declare no conflict of interest.

[1] D. Larcher, J.-M. Tarascon, *Nat. Chem.* **2015**, *7*, 19.

[2] S. Chen, Y. Su, P. Deng, R. Qi, J. Zhu, J. Chen, Z. Wang, L. Zhou, X. Guo, B. Y. Xia, *ACS Catal.* **2020**, *10*, 4640.

[3] F. Díaz-González, A. Sumper, O. Gomis-Bellmunt, R. Villafáfila-Robles, *Renewable Sustainable Energy Rev.* **2012**, *16*, 2154.

[4] P. Deng, H. Wang, R. Qi, J. Zhu, S. Chen, F. Yang, L. Zhou, K. Qi, H. Liu, B. Y. Xia, *ACS Catal.* **2020**, *10*, 743.

[5] H. D. Yoo, E. Markevich, G. Salitra, D. Sharon, D. Aurbach, *Mater. Today* **2014**, *17*, 110.

[6] D. Qian, C. Ma, K. L. More, Y. S. Meng, M. Chi, *NPG Asia Mater.* **2015**, *7*, e193.

[7] S.-W. Kim, H.-W. Lee, P. Muralidharan, D.-H. Seo, W.-S. Yoon, D. K. Kim, K. Kang, *Nano Res.* **2011**, *4*, 505.

[8] M. M. Rahman, I. Sultana, Z. Chen, M. Srikanth, L. H. Li, X. J. Dai, Y. Chen, *Nanoscale* **2015**, *7*, 13088.

[9] J. Lu, T. Wu, K. Amine, *Nat. Energy* **2017**, *2*, 17011.

[10] X. Li, H. Y. Wang, H. Yang, W. Cai, S. Liu, B. Liu, *Small Methods* **2018**, *2*, 1700395.

[11] J. D. Kirtley, D. M. Halat, M. D. McIntyre, B. C. Eigenbrodt, R. A. Walker, *Anal. Chem.* **2012**, *84*, 9745.

ADVANCED
SCIENCE NEWS
www.advancedsciencenews.com

ADVANCED
MATERIALS
TECHNOLOGIES
www.advmattechnol.de

[12] X. Cheng, M. Pecht, *Energies* **2017**, *10*, 591.

[13] M. Morcrette, Y. Chabre, G. Vaughan, G. Amatucci, J.-B. Leriche, S. Patoux, C. Masquelier, J. Tarascon, *Electrochim. Acta* **2002**, *47*, 3137.

[14] Y. Yuan, K. Amine, J. Lu, R. Shahbazian-Yassar, *Nat. Commun.* **2017**, *8*, 15806.

[15] H. Wang, R. G. Downing, J. A. Dura, D. S. Hussey, *Polymers for Energy Storage and Delivery: Polyelectrolytes for Batteries and Fuel Cells*, ACS Publications, Washington, DC **2012**, p. 91.

[16] S.-M. Bak, Z. Shadike, R. Lin, X. Yu, X.-Q. Yang, *NPG Asia Mater.* **2018**, *10*, 563.

[17] C.-M. Wang, *J. Mater. Res.* **2015**, *30*, 326.

[18] J. Oudenhoven, F. Labohm, M. Mulder, R. Niessen, F. Mulder, P. Notten, *Adv. Mater.* **2011**, *23*, 4103.

[19] R. Zhu, C. Liu, J. Feng, Z. Guo, *ECS Trans.* **2018**, *85*, 347.

[20] A. M. Tripathi, W.-N. Su, B. J. Hwang, *Chem. Soc. Rev.* **2018**, *47*, 736.

[21] P. Harks, F. Mulder, P. Notten, *J. Power Sources* **2015**, *288*, 92.

[22] C. Grey, J. Tarascon, *Nat. Mater.* **2017**, *16*, 45.

[23] M. W. Davidson, M. Abramowitz, *Encyclopedia of Imaging Science and Technology*, Wiley, New York **2002**.

[24] T. C. Kriss, V. M. Kriss, *Neurosurgery* **1998**, *42*, 899.

[25] R. Hooke, Micrographia: Or Some Physical Descriptions of Minute Bodies Made by Magnifying Glasses, with Observations and Inquiries Thereupon, Courier Corporation, Mineola, New York, USA **2003**.

[26] J. van Zuylen, *J. Microsc.* **1981**, *121*, 309.

[27] E. H. Stelzer, *Nature* **2002**, *417*, 806.

[28] B. R. Masters, *Opt. Photonics News* **2007**, *18*, 18.

[29] F. Zernike, *Physica* **1942**, *9*, 974.

[30] A. Pirie, D. M. Simpson, *Biochem. J.* **1946**, *40*, 14.

[31] R. J. Best, *Aust. J. Exp. Biol. Med. Sci.* **1944**, *22*, 223.

[32] O. Heimstiidt, *Z. Wiss. Mikrosk. Mikrosk. Tech.* **1911**, *28*, 330.

[33] A. H. Coons, M. H. Kaplan, *J. Exp. Med.* **1950**, *91*, 1.

[34] A. B. Cubitt, R. Heim, S. R. Adams, A. E. Boyd, L. A. Gross, R. Y. Tsien, *Trends Biochem. Sci.* **1995**, *20*, 448.

[35] M. Marvin, Google Patents, US3013467 A, **1961**.

[36] K. Ueno, M. Seo, *J. Electrochem. Soc.* **1999**, *146*, 1496.

[37] E. Chason, J. Floro, *MRS Online Proc. Libr. Arch.* **1996**, *428*, 499.

[38] S. Hearne, E. Chason, J. Han, J. Floro, J. Figiel, J. Hunter, H. Amano, I. Tsong, *Appl. Phys. Lett.* **1999**, *74*, 356.

[39] P. Costamagna, S. Srinivasan, *J. Power Sources* **2001**, *102*, 253.

[40] J. H. Nam, M. Kaviany, *Int. J. Heat Mass Transfer* **2003**, *46*, 4595.

[41] S. G. Kandlikar, Z. Lu, *Appl. Therm. Eng.* **2009**, *29*, 1276.

[42] K. Tüber, D. Pócza, C. Hebling, *J. Power Sources* **2003**, *124*, 403.

[43] D. Lee, J. Bae, *Int. J. Hydrogen Energy* **2012**, *37*, 422.

[44] R. Aslam, D. Ingham, M. Ismail, K. Hughes, L. Ma, M. Pourkashanian, *J. Energy Inst.* **2018**, *91*, 1057.

[45] F.-B. Weng, A. Su, C.-Y. Hsu, C.-Y. Lee, *J. Power Sources* **2006**, *157*, 674.

[46] D. Spernjak, A. K. Prasad, S. G. Advani, *J. Power Sources* **2010**, *195*, 3553.

[47] E. Kumbur, K. Sharp, M. Mench, *J. Power Sources* **2006**, *161*, 333.

[48] A. Hakenjos, H. Muenter, U. Wittstadt, C. Hebling, *J. Power Sources* **2004**, *131*, 213.

[49] D. Spernjak, A. K. Prasad, S. G. Advani, *J. Power Sources* **2007**, *170*, 334.

[50] H. Guo, X. Liu, J. F. Zhao, F. Ye, C. F. Ma, *Energy* **2016**, *112*, 926.

[51] Z. Zhan, C. Wang, W. Fu, M. Pan, *Int. J. Hydrogen Energy* **2012**, *37*, 1094.

[52] K. Sugiura, M. Nakata, T. Yodo, Y. Nishiguchi, M. Yamauchi, Y. Itoh, *J. Power Sources* **2005**, *145*, 526.

[53] I. S. Hussaini, C.-Y. Wang, *J. Power Sources* **2009**, *187*, 444.

[54] J. Sergi, **2010**.

[55] J. M. Sergi, S. G. Kandlikar, *Int. J. Hydrogen Energy* **2011**, *36*, 12381.

[56] R. Banerjee, S. G. Kandlikar, *J. Power Sources* **2014**, *247*, 9.

[57] A. Bozorgnezhad, M. Shams, H. Kanani, M. Hasheminasab, G. Ahmadi, *Int. J. Hydrogen Energy* **2015**, *40*, 2808.

[58] J. Borrelli, S. G. Kandlikar, T. Trabold, J. Owejan, presented at *International Conference on Nanochannels, Microchannels, and Minichannels*, Toronto, Ontario, Canada, June **2005**.

[59] T.-L. Liu, C. Pan, *J. Power Sources* **2012**, *207*, 60.

[60] J. H. Kang, K.-J. Lee, J. H. Nam, C.-J. Kim, H. S. Park, S. Lee, I. Kwang, *J. Power Sources* **2010**, *195*, 2608.

[61] J. W. Lichtman, J.-A. Conchello, *Nat. Methods* **2005**, *2*, 910.

[62] S. Litster, D. Sinton, N. Djilali, *J. Power Sources* **2006**, *154*, 95.

[63] A. Bazylak, D. Sinton, N. Djilali, *J. Power Sources* **2008**, *176*, 240.

[64] B. Gao, T. S. Steenhuis, Y. Zevi, J.-Y. Parlange, R. N. Carter, T. A. Trabold, *J. Power Sources* **2009**, *190*, 493.

[65] K. S. Kung, *Geoderma* **1990**, *46*, 59.

[66] N. McCarthy, R. Chen, G. Offer, R. Thring, *Int. J. Hydrogen Energy* **2016**, *41*, 17631.

[67] C. Zhu, F. V. Bright, W. A. Wyatt, G. M. Hieftje, *J. Electrochem. Soc.* **1989**, *136*, 567.

[68] Y. P. Patil, T. A. Seery, M. T. Shaw, R. S. Parnas, *Ind. Eng. Chem. Res.* **2005**, *44*, 6141.

[69] V. Prabhakaran, C. G. Arges, V. Ramani, *Proc. Natl. Acad. Sci. USA* **2012**, *109*, 1029.

[70] J. F. Botero-Cadavid, *Doctor of Philosophy Thesis*, University of Victoria, Canada **2014**.

[71] Y. Ishikawa, T. Morita, M. Shiozawa, *ECS Trans.* **2006**, *3*, 889.

[72] Y. Ishikawa, H. Hamada, M. Uehara, M. Shiozawa, *J. Power Sources* **2008**, *179*, 547.

[73] M. M. Daino, Z. Lu, J. LaManna, J. Owejan, T. Trabold, S. G. Kandlikar, *ECS Trans.* **2010**, *33*, 1423.

[74] Y. Wu, N. Liu, *Chem* **2018**, *4*, 438.

[75] G. Wan, F. Guo, H. Li, Y. Cao, X. Ai, J. Qian, Y. Li, H. Yang, *ACS Appl. Mater. Interfaces* **2018**, *10*, 593.

[76] L. Kong, Y. Xing, M. G. Pecht, *IEEE Access* **2018**, *6*, 8387.

[77] W.-S. Kim, W.-Y. Yoon, *Electrochim. Acta* **2004**, *50*, 541.

[78] H. Sano, H. Sakaebe, H. Matsumoto, *J. Power Sources* **2011**, *196*, 6663.

[79] H. Sano, H. Sakaebe, H. Matsumoto, *Electrochemistry* **2012**, *80*, 777.

[80] H. Sano, H. Sakaebe, H. Matsumoto, *Chem. Lett.* **2013**, *42*, 77.

[81] F. Sagane, K.-i. Ikeda, K. Okita, H. Sano, H. Sakaebe, Y. Iriyama, *J. Power Sources* **2013**, *233*, 34.

[82] J. Steiger, D. Kramer, R. Mönig, *J. Power Sources* **2014**, *261*, 112.

[83] J. Steiger, D. Kramer, R. Mönig, *Electrochim. Acta* **2014**, *136*, 529.

[84] J. Steiger, G. Richter, M. Wenk, D. Kramer, R. Mönig, *Electrochem. Commun.* **2015**, *50*, 11.

[85] P. Bai, J. Li, F. R. Brushett, M. Z. Bazant, *Energy Environ. Sci.* **2016**, *9*, 3221.

[86] A. Aryanfar, D. J. Brooks, A. J. Colussi, M. R. Hoffmann, *Phys. Chem. Chem. Phys.* **2014**, *16*, 24965.

[87] A. Aryanfar, T. Cheng, A. J. Colussi, B. V. Merinov, W. A. Goddard III, M. R. Hoffmann, *J. Chem. Phys.* **2015**, *143*, 134701.

[88] Z. Guo, J. Zhu, J. Feng, S. Du, *RSC Adv.* **2015**, *5*, 69514.

[89] C. Fear, T. Adhikary, R. E. Carter, A. N. Mistry, C. T. Love, P. P. Mukherjee, *ACS Appl. Mater. Interfaces* **2020**, *12*, 30438.

[90] T. Ding, *Master of Science Thesis*, University of Wisconsin Milwaukee, USA **2016**.

[91] J. Kuwabara, K. Sato, *ECS Trans.* **2017**, *75*, 47.

[92] H. B. Chew, B. Hou, X. Wang, S. Xia, *Int. J. Solids Struct.* **2014**, *51*, 4176.

[93] R. Koerver, W. Zhang, L. de Biasi, S. Schweidler, A. O. Kondrakov, S. Kolling, T. Brezesinski, P. Hartmann, W. G. Zeier, J. Janek, *Energy Environ. Sci.* **2018**, *11*, 2142.

[94] L. Beaulieu, V. Cumyn, K. Eberman, L. Krause, J. Dahn, *Rev. Sci. Instrum.* **2001**, *72*, 3313.

[95] L. Beaulieu, K. Eberman, R. Turner, L. Krause, J. Dahn, *Electrochem. Solid State Lett.* **2001**, *4*, A137.

2000555 (18 of 21)

**ADVANCED
SCIENCE NEWS**
www.advancedsciencenews.com

**ADVANCED
MATERIALS
TECHNOLOGIES**
www.advmattechnol.de

[96] A. Timmons, J. Dahn, *J. Electrochem. Soc.* **2007**, *154*, A444.

[97] K. Nishikawa, H. Munakata, K. Kanamura, *J. Power Sources* **2013**, *243*, 630.

[98] K. Dokko, N. Nakata, K. Kanamura, *J. Power Sources* **2009**, *189*, 783.

[99] K. Dokko, N. Nakata, Y. Suzuki, K. Kanamura, *J. Phys. Chem. C* **2010**, *114*, 8646.

[100] H. Munakata, B. Takemura, T. Saito, K. Kanamura, *J. Power Sources* **2012**, *217*, 444.

[101] K. Nishikawa, J. Moon, K. Kanamura, *J. Power Sources* **2016**, *302*, 46.

[102] X. H. Liu, L. Zhong, S. Huang, S. X. Mao, T. Zhu, J. Y. Huang, *ACS Nano* **2012**, *6*, 1522.

[103] S.-J. Lee, J.-K. Lee, S.-H. Chung, H.-Y. Lee, S.-M. Lee, H.-K. Baik, *J. Power Sources* **2001**, *97–98*, 191.

[104] V. A. Sethuraman, M. J. Chon, M. Shimshak, N. Van Winkle, P. R. Guduru, *Electrochem. Commun.* **2010**, *12*, 1614.

[105] V. A. Sethuraman, M. J. Chon, M. Shimshak, V. Srinivasan, P. R. Guduru, *J. Power Sources* **2010**, *195*, 5062.

[106] S. P. Nadimpalli, V. A. Sethuraman, G. Bucci, V. Srinivasan, A. F. Bower, P. R. Guduru, *J. Electrochem. Soc.* **2013**, *160*, A1885.

[107] V. A. Sethuraman, N. Van Winkle, D. P. Abraham, A. F. Bower, P. R. Guduru, *J. Power Sources* **2012**, *206*, 334.

[108] S. P. Nadimpalli, R. Tripuraneni, V. A. Sethuraman, *J. Electrochem. Soc.* **2015**, *162*, A2840.

[109] Z. Choi, D. Kramer, R. Mönig, *J. Power Sources* **2013**, *240*, 245.

[110] M. Pharr, Z. Suo, J. J. Vlassak, *Nano Lett.* **2013**, *13*, 5570.

[111] M. Pharr, Z. Suo, J. J. Vlassak, *J. Power Sources* **2014**, *270*, 569.

[112] Y. S. Choi, M. Pharr, K. H. Oh, J. J. Vlassak, *J. Power Sources* **2015**, *294*, 159.

[113] M. Pharr, Y. S. Choi, D. Lee, K. H. Oh, J. J. Vlassak, *J. Power Sources* **2016**, *304*, 164.

[114] W. Mao, Z. Wang, C. Li, X. Zhu, C. Dai, H. Yang, X. Chen, D. Fang, *J. Power Sources* **2018**, *402*, 272.

[115] C. Uhlmann, J. Illig, M. Ender, R. Schuster, E. Ivers-Tiffée, *J. Power Sources* **2015**, *279*, 428.

[116] P. Maire, A. Evans, H. Kaiser, W. Scheifele, P. Novák, *J. Electrochem. Soc.* **2008**, *155*, A862.

[117] P. Maire, H. Kaiser, W. Scheifele, P. Novák, *J. Electroanal. Chem.* **2010**, *644*, 127.

[118] S. J. Harris, A. Timmons, D. R. Baker, C. Monroe, *Chem. Phys. Lett.* **2010**, *485*, 265.

[119] K. E. Thomas-Alyea, C. Jung, R. B. Smith, M. Z. Bazant, *J. Electrochem. Soc.* **2017**, *164*, E3063.

[120] S. Bhattacharya, A. R. Riahi, A. T. Alpas, *Scr. Mater.* **2011**, *64*, 165.

[121] M. Otoyama, A. Sakuda, A. Hayashi, M. Tatsumisago, *Solid State Ionics* **2018**, *323*, 123.

[122] Y. Feng, M. Panagopoulou, A. Cheriet, B. M. Koo, C. Henry-de-Villeneuve, M. Rosso, F. Ozanam, *Electrochim. Acta* **2019**, *302*, 249.

[123] V. Roscher, K.-R. Riemschneider, presented at *2017 IEEE Sensors Applications Symposium (SAS)*, Glassboro, NJ, USA, March **2017**.

[124] J. Wan, W. Bao, Y. Liu, J. Dai, F. Shen, L. Zhou, X. Cai, D. Urban, Y. Li, K. Jungjohann, *Adv. Energy Mater.* **2015**, *5*, 1401742.

[125] M. Azhagurajan, T. Kajita, T. Itoh, Y.-G. Kim, K. Itaya, *J. Am. Chem. Soc.* **2016**, *138*, 3355.

[126] X. Yu, H. Pan, Y. Zhou, P. Northrup, J. Xiao, S. Bak, M. Liu, K. W. Nam, D. Qu, J. Liu, *Adv. Energy Mater.* **2015**, *5*, 1500072.

[127] Y. Sun, Z. W. Seh, W. Li, H. Yao, G. Zheng, Y. Cui, *Nano Energy* **2015**, *11*, 579.

[128] A. l. Jarry, S. b. Gottis, Y.-S. Yu, J. Roque-Rosell, C. Kim, J. Cabana, J. Kerr, R. Kostecki, *J. Am. Chem. Soc.* **2015**, *137*, 3533.

[129] Y. Qiao, Z. Zhou, Z. Chen, S. Du, Q. Cheng, H. Zhai, N. J. Fritz, Q. Du, Y. Yang, *Nano Energy* **2018**, *45*, 68.

[130] X. Ren, J. Wang, Z. Peng, L. Lu, *Chem. Sci.* **2018**, *9*, 231.

[131] N. A. Padilla, M. T. Rea, M. Foy, S. P. Upadhyay, K. A. Desrochers, T. Derus, K. A. Knapper, N. H. Hunter, S. Wood, D. A. Hinton, *ACS Sens.* **2017**, *2*, 903.

[132] J. Houser, J. Clement, A. Pezeshki, M. M. Mench, *J. Power Sources* **2016**, *302*, 369.

[133] A. A. Wong, M. J. Aziz, S. Rubinstein, *ECS Trans.* **2017**, *77*, 153.

[134] A. A. Wong, S. Rubinstein, M. J. Aziz, presented at *232nd ECS Meeting*, National Harbor, MD, October **2017**.

[135] J. Martin, P. Oshkai, N. Djilali, *J. Electrochem. Energy Convers. Storage* **2005**, *2*, 70.

[136] S. Burgmann, M. Blank, J. Wartmann, A. Heinzel, *Energy Procedia* **2012**, *28*, 88.

[137] J. Rubio-Garcia, A. Kucernak, A. Charleson, *Electrochem. Commun.* **2018**, *93*, 128.

[138] J. Diggle, A. Despic, J. M. Bockris, *J. Electrochem. Soc.* **1969**, *116*, 1503.

[139] R. Naybour, *Electrochim. Acta* **1968**, *13*, 763.

[140] C. P. Chen, J. Jorné, *J. Electrochem. Soc.* **1990**, *137*, 2047.

[141] Y. Oren, U. Landau, *Electrochim. Acta* **1982**, *27*, 739.

[142] S. J. Banik, R. Akolkar, *Electrochim. Acta* **2015**, *179*, 475.

[143] T. Minami, *Thin Solid Films* **2008**, *516*, 5822.

[144] M. Nishii, R. Sakurai, K. Sugie, Y. Masuda, R. Hattori, *SID Int. Symp. Dig. Tech. Pap.* **2009**, *40*, 768.

[145] L. Peng, X. Peng, B. Liu, C. Wu, Y. Xie, G. Yu, *Nano Lett.* **2013**, *13*, 2151.

[146] S. Yu, W. Yang, L. Li, W. Zhang, *Sol. Energy Mater. Sol. Cells* **2016**, *144*, 652.

[147] J. Wan, F. Gu, W. Bao, J. Dai, F. Shen, W. Luo, X. Han, D. Urban, L. Hu, *Nano Lett.* **2015**, *15*, 3763.

[148] Y. Seekaew, O. Arayawut, K. Timsorn, C. Wongchoosuk, *Carbon-Based Nanofillers and Their Rubber Nanocomposites*, Elsevier, Amsterdam **2019**, p. 259.

[149] Y. Ma, L. Zhi, *Small Methods* **2019**, *3*, 1800199.

[150] C. Xiang, M. Li, M. Zhi, A. Manivannan, N. Wu, *J. Power Sources* **2013**, *226*, 65.

[151] S. Shashkova, M. C. Leake, *Biosci. Rep.* **2017**, *37*, BSR20170031.

[152] B. Rotman, *Proc. Natl. Acad. Sci. USA* **1961**, *47*, 1981.

[153] B. Rotman, *Fluorescence Techniques in Cell Biology*, Springer, Berlin **1973**, p. 333.

[154] L. Edman, Z. Földes-Papp, S. Wennmalm, R. Rigler, *Chem. Phys.* **1999**, *247*, 11.

[155] M. B. Roeffaers, B. F. Sels, H. Uji-i, F. C. De Schryver, P. A. Jacobs, D. E. De Vos, J. Hofkens, *Nature* **2006**, *439*, 572.

[156] K. Naito, T. Tachikawa, M. Fujitsuka, T. Majima, *J. Phys. Chem. C* **2008**, *112*, 1048.

[157] W. Xu, J. S. Kong, P. Chen, *Phys. Chem. Chem. Phys.* **2009**, *11*, 2767.

[158] W. Xu, H. Shen, Y. J. Kim, X. Zhou, G. Liu, J. Park, P. Chen, *Nano Lett.* **2009**, *9*, 3968.

[159] W. Xu, J. S. Kong, Y.-T. E. Yeh, P. Chen, *Nat. Mater.* **2008**, *7*, 992.

[160] X. Zhou, W. Xu, G. Liu, D. Panda, P. Chen, *J. Am. Chem. Soc.* **2010**, *132*, 138.

[161] K. S. Han, G. Liu, X. Zhou, R. E. Medina, P. Chen, *Nano Lett.* **2012**, *12*, 1253.

[162] M. A. Ochoa, X. Zhou, P. Chen, R. F. Loring, *J. Chem. Phys.* **2011**, *135*, 174509.

[163] X. Zhou, N. M. Andoy, G. Liu, E. Choudhary, K.-S. Han, H. Shen, P. Chen, *Nat. Nanotechnol.* **2012**, *7*, 237.

[164] N. M. Andoy, X. Zhou, E. Choudhary, H. Shen, G. Liu, P. Chen, *J. Am. Chem. Soc.* **2013**, *135*, 1845.

[165] P. Chen, X. Zhou, N. M. Andoy, K.-S. Han, E. Choudhary, N. Zou, G. Chen, H. Shen, *Chem. Soc. Rev.* **2014**, *43*, 1107.

[166] E. J. Peterman, H. Sosa, W. Moerner, *Annu. Rev. Phys. Chem.* **2004**, *55*, 79.

**ADVANCED
SCIENCE NEWS**

www.advancedsciencenews.com

**ADVANCED
MATERIALS
TECHNOLOGIES**

www.advmattechnol.de

Binbin Chen is currently a research associate in Imperial College London. Having graduated from University of Science and Technology of China in 2012 with a B.Sc. degree in modern mechanics, Binbin undertook his Ph.D. research on batteries at the University of Hong Kong and completed it in 2017. Prior to joining Imperial College London, he was a senior battery engineer in ASTRI Hong Kong, responsible for developing commercial Li-ion and Zn-ion batteries. His expertise lies in design, manufacturing, and characterization of battery devices including Li-ion batteries, metal–air batteries, and multivalent-ion batteries.
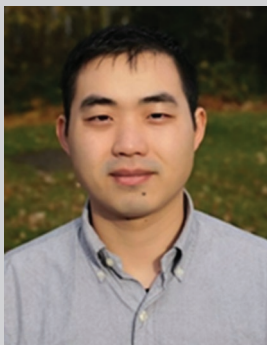
Hao Zhang obtained his Ph.D. degree with the topic of chemical and mechanical engineering from East China University of Science and Technology in 2015. He is currently a research associate at the School of Engineering, The University of Edinburgh. His research interest lies in sustainable and renewable energy solutions through electrochemical and photoelectrochemical approaches. He is also interested in the recovery of precious energy materials to develop low cost and sustainable energy devices.

Jin Xuan graduated with a Ph.D. degree from The University of Hong Kong in 2012, with research topic in energy and environment engineering. He is currently a professor and the Head of Department of Chemical Engineering in Loughborough University. Professor Xuan's research focuses on the clean growth, industrial decarbonization, and sustainable development via engineering innovations in solar fuels, CCUS, hydrogen and fuel cells, e-synthesis, etc. He is passionate about developing and applying bespoke AI and digital solutions to enable next-generation energy and chemical devices, processes, and systems.

Gregory Offer is a reader in the Department of Mechanical Engineering, Imperial College London, and his research is based around fuel cell, battery and supercapacitor technology, and their application, mostly in transport, from the fundamental science to integration and systems engineering. The problems he investigates tend to emerge at the interface between the science and engineering.

**ADVANCED
SCIENCE NEWS**

www.advancedsciencenews.com

**ADVANCED
MATERIALS
TECHNOLOGIES**

www.advmattechnol.de

Huizhi Wang is a lecturer in the Department of Mechanical Engineering and a member of the Electrochemical Science & Engineering Group in Imperial College London. She received her Ph.D. in mechanical engineering from the University of Hong Kong in 2012. Her research interest lies in electrochemical energy engineering with a particular focus on the thermofluid aspects of electrochemical energy conversion and storage systems including fuel cells, batteries and electrolysers. She is also interested in advanced manufacturing (e.g., microfluidic-based fabrication, additive manufacturing) and diagnostic techniques for electrochemical energy applications.